LEAD ARTICLE

Acta Cryst. (1996). A52, 11–41

The Analysis and Interpretation of Neutron and X-ray Specular Reflection

J. R. LU, E. M. LEE AND R. K. THOMAS*

Physical Chemistry Laboratory, South Parks Road, Oxford OX1 3QZ, England. E-mail: thomas@vax.ox.ac.uk

(Received 6 March 1995; accepted 10 August 1995)

Abstract

Methods of analysing neutron and X-ray specular reflection from interfacial systems are reviewed. Normally, the profile of the scattering-length density is determined in such experiments but here particular emphasis is given to the determination of the interfacial composition profile using partial structure factors and simultaneous fitting of sets of reflectivity profiles from a given structure, obtained either by isotopic substitution or by the use of neutrons and X-rays together. Aspects of the analysis of reflectivity data in terms of the resolution of the experiment, the phase problem and the possible ways of describing the structure of an interface are considered with reference to an unusually large set of independent data from isotopic species of a monolayer of hexadecyltrimethylammonium bromide adsorbed at the air/water interface. Data from another surfactant, the monododecyl ether of triethylene glycol, is used to assess the optimum choice of isotopic composition for combining a single set of neutron data with an X-ray reflectivity profile from an adsorbed layer at the air/water interface.

Dr E. M. Lee's doctorate was the first application of neutron reflection to the study of the structure of a surfactant at the air/liquid interface. Since then, she has worked on ionomer membranes and has more recently, while a Glasstone Fellow at Oxford University, been developing the use of neutron reflection to study the interaction of charged species at surfaces.

After obtaining his first degree at the Petroleum University in the People's Republic of China, Dr J. R. Lu obtained his doctorate at Hull University under the supervision of Professor Aveyard. For the last five years, he has been working at the University of Oxford developing and applying the technique of neutron reflection to amphiphiles adsorbed at interfaces.

Dr R. K. Thomas has been applying neutron scattering and X-ray techniques to a variety of surface problems for 20 years. Since proposing in a paper published in 1981 that neutron reflection would be a sensitive technique for investigating surface structure, he has been developing and applying this technique, particularly to the absorption of surfactants and polymers at wet interfaces. He has been at the University of Oxford, where he is currently a lecturer, during the whole of this period.

1. Introduction

Specular reflection of either X-rays or neutrons is now an established technique for investigating the structure of thin films and interfaces. The experiment is relatively straightforward in execution but the analysis and interpretation are more difficult and have therefore been given rather more attention. There are three main problems in the analysis, the most obvious being the phase problem, present in all scattering experiments. For neutrons, there is also the problem of the small range of momentum transfer covered by the experiment, which puts a limit on the resolution. Together, these two factors may lead to ambiguity in the interpretation. The further problem is that what is derived from a successful analysis is the scattering-length-density profile normal to the interface and there may be ambiguities in the interpretation of this profile to obtain the distribution of the various components through the interface.

We review these three problems in this paper and attempt to show that the partial-structure-factor method of analysing the reflectivity goes some way to solving the third of these problems and, in doing so, can, at least partially, solve the first two problems. We review the basic theory of the specular reflectivity experiment and the variety of the methods that have been used to solve one or other of the problems above. We then outline the partial-structure-factor method and apply it to a set of experimental results on a surfactant adsorbed at the air/liquid interface, which have already been published, in two ways. In the first, we determine the partial structure factors from the data and then fit them with a set of structural parameters. This is the method that we have developed and applied on a number of occasions (Crowley, Lee, Simister & Thomas, 1991; Lu, Hromadova, Simister, Thomas & Penfold, 1994; Lu, Hromadova & Thomas, 1993; Lu, Li, Smallwood, Thomas & Penfold, 1995; Lu, Li, Su, Thomas & Penfold, 1993; Lu *et al.*, 1994; Lu, Li, Thomas, Staples, Tucker & Penfold. 1993; Lu, Simister, Lee, Thomas, Rennie & Penfold, 1992; Lu, Simister, Thomas & Penfold, 1993*a*; Simister, Lee, Thomas & Penfold, 1992*a*,*b*). In the second fitting procedure, we use analytic expressions for the partial structure factors but fit the structural parameters of the layer to the whole set of reflectivity

data by least squares. This method has recently been described by Lee & Milnes (1995) but is used here to fit simultaneously a wider range of independent reflectivity profiles from a single structure. The overdetermination of the structure is used to demonstrate some of the choices of isotopic labelling for the determination of layer structure in reflection experiments. We also attempt to give an overview of the possible options for interpreting specular reflectivity data and to explore the resolution limit of the neutron experiment. The main emphasis is on results from neutron reflection but some consideration is given to X-ray experiments particularly when there are advantages in combining the two techniques.

2. Theory of specular reflection

The unusual feature of specular reflectivity, when compared with other forms of scattering, particularly small-angle scattering, is that it may be calculated exactly, however complicated the interface, provided that the interface is uniform in its plane. The method of calculation is either to use an analytic formula for the reflectivity if the structure of the interface is simple or to compute it using the optical matrix method. Comparison of reflectivity profiles calculated from different models with observed reflectivities cannot be guaranteed to give a unique solution and it may then be a better procedure to use approximate calculations of the reflectivity for which there is a direct relation between reflectivity and structure. This is part of the reason for using the kinematic approximation for the reflectivity, which relates the reflectivity to the interfacial scattering-length-density profile *via* the squared modulus of a Fourier transform. In order to illustrate the different approaches and to analyse some of the claims that have been made about uniqueness, we will start by considering the simplest possible model of an interface, a single uniform layer on a substrate, in some detail. The main purpose of the paper is to demonstrate the power of the partial-structure-factor method, which operates within the framework of the kinematic approximation. It is helpful to be able to set this method and several other approaches that use the kinematic approximation in the context of the more exact optical matrix calculation, so we start by outlining the latter.

Fig. 1 gives a breakdown of the specular reflection of light from a uniform monolayer. The reflected wave is a sum of the primary, secondary *etc.* waves, labelled (*a*), (*b*) *etc.* In terms of the Fresnel reflection and transmission coefficients r_{ij} and t_{ij} (Born & Wolf, 1970), the amplitude of the reflected beam is

$$\mathbf{R} = r_{01} + t_{01}r_{12}t_{10}\exp(2i\beta_1) + t_{01}r_{12}r_{10}r_{12}t_{10}\exp(4i\beta_1) + \ldots, \quad (1)$$

where β_1 is the phase shift on traversing the layer once and equals $q_1\tau_1 \sin\theta$, where q_1 is the wave vector of the radiation normal to the interface in layer 1. Equation (1) is a geometric series that reduces to

$$\mathbf{R} = \frac{r_{01} + r_{12}\exp(2i\beta_1)}{1 + r_{01}r_{12}\exp(2i\beta_1)}, \quad (2)$$

where we have made use of simple relations between r and t (Born & Wolf, 1970). The reflectivity is just the squared amplitude of (2):

$$R = |\mathbf{R}|^2 = \frac{r_{01}^2 + r_{12}^2 + 2r_{01}r_{12}\cos(2\beta_1)}{1 + r_{01}^2r_{12}^2 + 2r_{01}r_{12}\cos(2\beta_1)}. \quad (3)$$

At angles greater than the critical angle, the Fresnel reflection coefficient for the electromagnetic s wave is (Born & Wolf, 1970)

$$r_{ij} = (q_i - q_j)/(q_i + q_j), \quad (4)$$

where q_i is the wave vector normal to the interface in layer i as before. For the smooth surface, the reflectivity is just

$$R = |\mathbf{R}|^2 = r_{01}^2. \quad (5)$$

In optics, it is convenient to work in terms of the refractive index and angle of incidence and the reflection coefficients are therefore expressed in terms of those quantities. For neutron and X-ray reflectivity, it is more convenient to work with the scattering-length density and momentum transfer. The relation between the refractive index and the scattering-length density is obtained by comparison of the solution of Schrödinger's equation for neutrons and the derivation of the optical reflectivity (Lekner, 1987, 1991) and is

$$n^2 = 1 - (\lambda^2/\pi)\rho, \quad (6)$$

where n is the refractive index, λ is the wavelength and ρ is the scattering-length density given by

$$\rho(z) = \sum_j b_j n_j(z), \quad (7)$$

where b_j is the scattering length and n_j is the number density of atomic species j. The neutron scattering length is an empirically determined number and the success

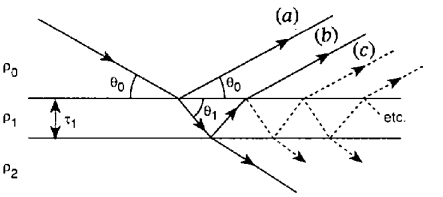

Fig. 1. The specular reflection of radiation from a monolayer on a substrate.

of many neutron experiments depends on it varying erratically through the Periodic Table and most particularly often varying sharply from isotope to isotope. We shall make extensive use of the difference between the different scattering of the isotopes of hydrogen for which $b_H = -3.74 \times 10^{-5}$ Å and $b_D = 6.67 \times 10^{-5}$ Å. For X-rays, b_j is replaced by $f_j e^2/mc^2$, where f_j is the atomic form factor, c is the speed of light, e and m are the charge and mass of the electron, and therefore X-ray scattering lengths increase steadily down the Periodic Table.

Schrödinger's equation for neutrons in a medium is (Lekner, 1987, 1991)

$$d^2\psi/dz^2 + q^2\psi = 0, \tag{8}$$

where q, the wave vector of the neutrons in the normal direction, is given by

$$q^2 = (2m/h^2)(E - V) - k_x^2, \tag{9}$$

where h is Planck's constant, k_x is the wave vector parallel to the surface and V is the potential energy given by

$$V = (h^2/2\pi m)\rho,$$

where ρ is the scattering-length density defined by (7). Continuity of ψ and $d\psi/dz$ gives (4) for the reflected amplitude at a sharp interface demonstrating the equivalence of the optical equations for the s-polarized wave and Schrödinger's equation. Equation (9) gives

$$q_i^2 - q_j^2 = 4\pi(\rho_j - \rho_i). \tag{10}$$

The momentum transfer κ is defined in terms of the grazing angle of incidence by

$$\kappa = (4\pi \sin\theta)/\lambda = 2q_0 \tag{11}$$

and the momentum transfer at which total reflection occurs between layers i and $i+1$ is then given by

$$\kappa_{ci}^2 = 4q_{ci}^2 = 16\pi(\rho_{i+1} - \rho_i) \tag{12}$$

using (10) with $q_j = 0$.

Using (4), (10) and (12), the reflectivity of the smooth surface is

$$R = r_{12}^2 = \kappa_c^4/[\kappa + (\kappa^2 - \kappa_c^2)^{1/2}]^4. \tag{13}$$

Many measurements are, however, done at values of κ much larger than κ_c when, using (12), (13) becomes

$$R \simeq 16\pi^2 \Delta\rho/\kappa^4, \tag{14}$$

which is the same as that derived directly from the kinematic approximation (see below). For the uniform monolayer, we use the optical equation (3), which with (4) and (10) and the further approximation that κ_c can be neglected in comparison with κ becomes

$$R \simeq (\rho_1 - \rho_0)^2 + (\rho_2 - \rho_1)^2 + 2(\rho_1 - \rho_0)(\rho_2 - \rho_1)\cos(\kappa\tau_1). \tag{15}$$

The basis of the calculation of the reflectivity using the optical matrix method is that the interface is divided into as many uniform layers as are necessary to describe the refractive-index profile normal to the surface with adequate resolution. The application of Maxwell's equations at each boundary leads to a characteristic 2×2 matrix for each layer. These matrices are multiplied successively and the reflected amplitude is extracted from the resulting 2×2 matrix. For light, there are large differences between the reflectivities for light polarized parallel or perpendicular to the reflection plane but at the low grazing angles of incidence characteristic of X-ray reflectivity there is negligible difference between the reflectivities of the two components and it is only necessary to calculate the reflectivity for one component. The reflection of neutrons is identical to the reflection of electromagnetic radiation polarized perpendicular (s wave) to the reflection plane.

The characteristic matrix for each component layer is given by

$$[M_j] = \begin{bmatrix} \cos\beta_j & -(i/q_j)\sin\beta_j \\ -iq_j\sin\beta_j & \cos\beta_j \end{bmatrix}, \tag{16}$$

where q_j and β_j are as defined in (1) and (4). The characteristic matrices for the various component layers are multiplied together and the reflected amplitude is given by

$$\mathbf{R} = \frac{(M_{11} + M_{12}q_{n+1})q_0 - (M_{21} + M_{22})q_{n+1}}{(M_{11} + M_{12}q_{n+1})q_0 + (M_{21} + M_{22})q_{n+1}}, \tag{17}$$

where M_{ij} are the elements of the final 2×2 matrix and q_0 and q_{n+1} refer to the initial and bulk phases. The two equations above are not the most convenient way of computing the reflectivity and recurrence relations between the Fresnel coefficients (Heavens, 1965; Parratt, 1954) are usually used to speed up the calculation.

There are two main difficulties in using the optical matrix method to analyse real data. One is that it may require a large number of component layers to describe the whole interface and the other is that when the layer scheme is complex it becomes difficult to relate the component layer scattering-length densities of isotopically different, but chemically identical, systems. There are a number of devices that solve the former problem, for example by the introduction of roughness into the matrix (Cowley & Ryan, 1987; Nevot & Croce, 1980) or by using a matrix where there are linear gradations of the scattering-length density between successive layers (Lekner, 1987). There is at present no easy solution of the second problem within the optical matrix framework, although it is readily dealt with in the kinematic approximation.

In the kinematic approximation, the reflectivity is given by (Als-Nielsen, 1985; Crowley, 1984)

$$\begin{aligned} R &= (16\pi^2/\kappa^2)|\rho(\kappa)|^2 \\ &= (16\pi^2/\kappa^4)|\rho^{(1)}(\kappa)|^2 \\ &= (16\pi^2/\kappa^2)P(\kappa) \\ &= (16\pi^2/\kappa^4)P^{(1)}(\kappa), \end{aligned} \tag{18}$$

where $\rho(\kappa)$ and $\rho^{(1)}(\kappa)$ are, respectively, the one-dimensional Fourier transforms of the scattering-length-density profile normal to the interface, $\rho(z)$, and its gradient, $\mathrm{d}\rho(z)/\mathrm{d}z$,

$$\rho(\kappa) = \int_{-\infty}^{\infty} \rho(z) \exp(-i\kappa z)\, \mathrm{d}z \tag{19}$$

and

$$\rho^{(1)}(\kappa) = \int_{-\infty}^{\infty} [\mathrm{d}\rho(z)/\mathrm{d}z] \exp(-i\kappa z)\, \mathrm{d}z. \tag{20}$$

The simple relation between the Fourier transforms of the scattering-length density and its differential results because we are considering profiles in only one dimension. The Fourier transforms of $|\rho(\kappa)|^2$ and $|\rho^{(1)}(\kappa)|^2$ are one-dimensional Patterson functions, $P(z)$ and $P^{(1)}(z)$, of the scattering-length-density profile, for example,

$$P(z) = \int_{-\infty}^{\infty} \rho(u)\rho(u-z)\, \mathrm{d}u. \tag{21}$$

There are a number of useful results that can be derived using (18), which we will use extensively below. The profile normal to a perfectly smooth interface is just the Heaviside function, the Fourier transform of whose Patterson is $\Delta\rho/\kappa^2$, which gives (14), already derived as an approximation above. The reflectivity for a single uniform monolayer on a substrate is also easily derived and $P^{(1)}(\kappa)$ is

$$\begin{aligned} P^{(1)}(\kappa) = {} & (\rho_1 - \rho_0)^2 + (\rho_2 - \rho_1)^2 \\ & + 2(\rho_1 - \rho_0)(\rho_2 - \rho_1)\cos(\kappa\tau_1) \end{aligned} \tag{22}$$

giving (15) above. An important case in neutron reflection experiments arises when $\rho_0 = \rho_2 = 0$ when

$$P^{(1)}(\kappa) = 4\rho_1^2 \sin^2(\kappa\tau_1). \tag{23}$$

Other distributions, which may be appropriate descriptions of interfacial distributions, are the Gaussian profile

$$\rho = \rho_0 \exp(-4z^2/\sigma^2), \tag{24}$$

where σ is the full width at $1/e$ of the maximum and which is a symmetrical distribution, and the tanh profile

$$\rho = \rho_0 \left[\tfrac{1}{2} + \tfrac{1}{2}\tanh(z/\zeta)\right], \tag{25}$$

which is an unsymmetrical distribution suitable for describing a solvent at the air/liquid interface and characterized by a width parameter ζ. The Fourier transform of (24) leads to

$$P^{(1)}(\kappa) = [(\pi\sigma^2\rho_0^2\kappa^2)/4] \exp(-\kappa^2\sigma^2) \tag{26}$$

and (25) to

$$P^{(1)}(\kappa) = \rho_0^2(\zeta\pi\kappa/2)^2 \operatorname{cosech}^2(\zeta\pi\kappa/2). \tag{27}$$

A further model, often used to describe the effects of capillary wave roughness on the solvent/air interface, is (Braslau, Deutsch, Pershan, Weiss, Als-Nielsen & Bohr, 1985)

$$P^{(1)}(\kappa) = \rho_0^2 \exp(-\sigma^2\kappa^2). \tag{28}$$

It is not strictly appropriate to compare (28) and (27) because the latter describes diffuseness and the former roughness (see §6 *Roughness*). However, specular reflection on its own cannot distinguish the two and it is then useful to be able to compare the significance of the two parameters σ and ζ. Expansion of the two expressions and comparison of the two linear terms shows that, in the linear region,

$$\sigma^2 \equiv (\zeta\pi)^2/12. \tag{29}$$

The limitations of the kinematic approximation and methods of improving the approximation have been discussed by many authors and we do not attempt a comprehensive survey here. The motivation behind these attempts is always linked to the possibility of inverting the data to obtain a unique solution for the structure and the Fourier transform offers the most obvious route to achieve this result. The most complete discussion of the kinematic approximation is given by Sears (1989) and improvements to the approximation, which would allow it to be used much closer to the critical angle, have been given by, amongst others, Sanyal *et al.* (1993) and Crowley (1993). The success of these approximations depends on the accuracy required and on how close to the critical angle the data are being analysed. The simplest procedure, and one used by several authors, is to divide the observed reflectivity by the exact reflectivity of the perfectly smooth uniform liquid that would give the same total reflection angle as the system in question. For a single uniform monolayer on a substrate and using the labelling of Fig. 1, this is equivalent to dividing (3) by (13) but with κ_c in the latter given by (12) with $(\rho_2 - \rho_0)$. This prevents the large divergence between (13) and (14) that occurs as $\kappa \rightarrow \kappa_c$. In Crowley's formalism (Crowley, 1993), the observed reflectivity is corrected according to the equation

$$\begin{aligned} &\{[1 + (1 - \kappa_c^2/\kappa^2)^{1/2}]/2\}^2[(R_{\mathrm{obs}} - R_f)/(1 - R_f)] \\ &\quad = R - R_k, \end{aligned} \tag{30}$$

where R_f is the exact reflectivity for the smooth interface [(13)], R_k is the kinematic reflectivity for the smooth interface [(14)] and R is the corrected reflectivity. Equation (30) is effective at an accuracy that is sufficient for most experimental data (Lu, Simister, Lee, Thomas, Rennie & Penfold, 1992) except possibly larger-scale structures where the most important information is close to the critical angle.

More attention has been given to improving the kinematic approximation because of the possibility of inversion through the Fourier transform than to developing other approximations. However, not only are there some exact analytic formula for special cases but there are also other approximate formulae. Several of the exact formulae are discussed in detail by Lekner (1987) and a formula of particular interest, because it applies to the exponent of the volume fraction distribution of a polymer at an interface, has been derived by Dietrich & Schack (1987) and applied successfully by Guiselin, Lee, Farnoux & Lapp (1991) to poly(dimethyl siloxane) adsorbed at the toluene/vapour interface. Lekner also discusses a number of approximate formulae and an approximate formula has been obtained by Zhou, Chen & Felcher (1992). None of these formulae is relevant to the problem which is the main concern of this paper and we do not consider them further here.

3. Methods of data analysis

The most common method for analysing data is to guess a model structure, calculate the exact reflectivity using the optical matrix method and compare the calculated and observed profiles. Because of the relatively low resolution of the experiment, a model structure typically consists of one to three uniform layers and roughness may or may not be included. Examples can be found in reviews by Penfold & Thomas (1990), Russell (1990), Schlossman & Pershan (1992) and Thomas (1995) and in most papers on reflectivity, either X-ray or neutron. The comparison may be done by eye, but least-squares fitting is also widely used. The quite different response of different parts of the profile to different structural features, the contribution of a significant background, the common presence of small systematic errors, and the presence of several local minima, all combined with the variation of the reflectivity over several orders of magnitude, often undermine the apparent objectivity of a least-squares analysis. It is also not easy to use simultaneous least-squares fitting when more than one reflectivity is available for a given structure, *e.g.* because of isotopic substitution or because both X-ray and neutron profiles have been measured. Most researchers with experience of attempting such fits will say that the problem is not to find a unique structure that will fit the data but to find *any* structure that will fit the data. To the authors' knowledge there are no results in the literature that have yet been shown to be substantially incorrect because of non-uniqueness of the fit. Although not usually explicitly used, much of the possible ambiguity is removed by constraints imposed by knowledge of some of the parameters of the system, the most powerful of which is often nothing more than the stoichiometry of the components at the interface. An example where this is a vital and explicit part of the analysis is given by Styrkas, Thomas, Adib, Davis, Hodge & Liu (1994). A common fault of model fitting is that results are often overinterpreted in terms of the experimental resolution actually available and there are also several examples of what are probably incorrect structures because of experimental errors in the measured reflectivity profiles, for example because the interface may be unexpectedly contaminated. Although errors arising from the analysis itself do not seem to be a serious issue, there is nevertheless a strong feeling that the analysis should be made less model dependent. There are three alternatives; the route that uses a model structure to fit the data, for example, the optical matrix method, as above, but seeks to introduce some objective criteria for the parameter set, the route that attempts to invert the data and thereby obtain a unique scattering-length-density profile, and the route that seeks to fit exact analytic formulae to the reflectivity in special circumstances. The division between the first two is somewhat arbitrary but we retain it for the moment.

3.1. *Objective criteria*

The simplest way to model an arbitrary scattering-length-density profile normal to an interface is to divide it up into a series of uniform layers or blocks. Some of the information about the thickness and composition of these blocks will come from the fitting of the reflectivity profile and some from other *prior* knowledge of the system. Obviously, the more the interface is subdivided into blocks, the more fitting parameters and the better the fit. The difficult choice is to decide at what point the addition of another block, although it will always improve the quality of the fit to the observed reflectivity, represents genuine new information about the system. The most complete discussion of this problem has been given by Sivia, Hamilton & Smith (1991) who have used Bayesian analysis to solve it. The reflectivity is fitted with 1, 2, 3 *etc.* layers and the fit progressively improves as more layers are added. The Bayesian analysis shows that the optimal value for N (the number of layers) is determined by a balance between the requirement for fitting the data adequately and a probabilistic preference for simplicity. Sivia *et al.* produce a quantitative criterion that combines the solution becoming less probable as the number of component layers increases with the improved fit as N increases. As put by Sivia *et al.*, 'this amounts to a quantitative statement of Ockam's Razor'. For a full discussion with good illustrative examples, the reader is referred to the original paper. What we note in passing

here is that the Sivia method essentially gives a means of fitting a reflectivity profile in terms of an optimum number of uniform layers. When the true profile is better described in terms of a smoothly varying scattering-length density, *i.e.* it must be described in terms of a relatively large number of uniform layers, it becomes difficult to use a method where the number of layers is optimized.

Related to the maximum-entropy method of Sivia *et al.* is the simulated annealing technique used by Kunz, Reiter, Götzelmann & Stamm (1993). As alluded to above, the main problem of least-squares fitting using the optical matrix calculation is the large number of local minima and simulated annealing is very effective at overcoming this problem and finding the global minimum. Kunz *et al.*'s program can also incorporate information other than from reflectivity, which helps to resolve the ambiguities inherent in any calculation based on fitting a model structure.

In the method of Sivia *et al.*, no attempt is made to divide the system into uniform layers of its chemical components, the presumption being that it would be more appropriate to infer the detailed structure from the optimum scattering-length-density profile. In many cases, especially those concerning monolayer adsorption, authors prefer to make the structural divisions at the outset and then to manipulate the chemical structure to obtain the best fit, *i.e.* they build in as much *a priori* knowledge as possible. We will consider an example of this below for hexadecyltrimethylammonium bromide (C_{16}TAB) but first we discuss an application of the logical limit of the structural description.

Denton, Gray & Sullivan (1994) have used a much finer subdivision of the interface together with more physically realistic distributions for the fragments than the usual block models and gain some advantage from this procedure. They calculate the reflectivity using the kinematic approximation, which is a limitation we discuss further below, and they have applied the method to the set of neutron reflectivities from isotopes of the surfactant, tetradecyltrimethylammonium bromide [$C_{14}H_{29}N(CH_3)_3Br$, abbreviated to C_{14}TAB], which adsorbs to form a monomolecular layer at the air/water interface. They divide the surfactant molecule into CH_2 fragments and assume that, since the distribution of each CH_2 fragment in the surfactant chain is determined by the roughness of the layer as a whole, each distribution should be described by the same function (this is discussed in some detail below). The scattering-length-density distribution for the whole chain may then be expressed in terms of this distribution function and the separation of the CH_2 fragments along the chain. This is then fitted by least squares to a set of isotopic data using a Gaussian distribution for the fragments (24), a tanh distribution for the water (25) and various choices for the tilt angles of successive fragments from the surface normal. Although the data being fitted do not apparently warrant such a fine subdivision, because in the original experiment the chain was only labelled as a complete fragment, the procedure nevertheless gives a more realistic and useful picture of the interface than the two-uniform-block model that has often been used to fit this kind of data. Thus, the main structural parameters derived are the tilt of the chain and the contribution of roughness to the thickness of the interface. The method is closely related to the partial-structure-factor method to be described below and we defer further discussion until then.

3.2. *Inversion*

The most obvious difficulty in the inversion of reflectivity data by Fourier transformation is the phase ambiguity inherent in (18). There are other issues [see, for example, the discussion in ch. 9 of Lekner (1987)] but by far the most important for reflectivity are the phase problem and the limited range of momentum transfer. Apart from special cases where the phase problem is soluble, *e.g.* for a causal monotonic scattering-length-density profile (Crowley, Lee, Simister, Thomas, Penfold & Rennie, 1990), there are essentially four ways of solving the phase problem:

(i) to make use of the non-linearity in the exact calculation of the reflectivity;

(ii) to use a technique that will determine the phase of $\rho^{(1)}(\kappa)$ separately from the amplitude;

(iii) to generate phase relationships between parts of the reflectivity profile by making some plausible assumptions about the nature of $\rho(z)$;

(iv) to use two or more different reflectivity profiles from the same system, *i.e.* X-ray and neutron, neutron profiles from different states of magnetization, X-ray

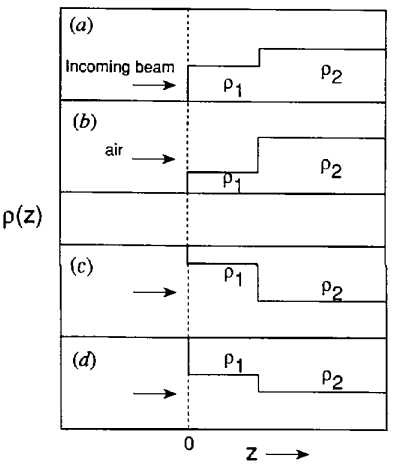

Fig. 2. The simplest set of scattering-length-density profiles across an interface that lead to the same reflectivity profile within the kinematic approximation.

profiles at different wavelengths across an absorption edge or neutron profiles with different isotopes.

We start by discussing a simple structure that gives rise to ambiguity in the kinematic approximation. Two examples have been given that demonstrate this clearly (Crowley, Lee, Simister & Thomas, 1991; Sivia, Hamilton & Smith, 1991) and we consider the first of these here because of its relevance to the method of inversion of Zhou & Chen (1993) (see also Zhou, Lee, Chen & Strey, 1992; Zhou & Chen, 1995). This model, shown in Fig. 2, corresponds to a commonly occurring case in actual experiments. In the kinematic approximation, the reflectivity of a uniform layer is given by (15) and it is clear that there are four possible sets of scattering-length density that will satisfy the equation; $(\rho_1 - \rho_0)$ and $(\rho_2 - \rho_1)$ may be interchanged and their signs may be changed. Although only small negative values of the scattering-length densities are possible in neutron scattering and not at all possible for X-rays, the two situations shown in Figs. 2(*c*) and (*d*) can occur in reflection at the solid/liquid interface because it is the value of the scattering-length density relative to that of the initial bulk phase that is important. Usually, the known physical properties of the bulk phases will be sufficient to discriminate between the (*a*)/(*b*) and (*c*)/(*d*) pairs in Fig. 2 but the general situation is that there is a phase problem at the level of the kinematic approximation. However, as pointed out by Zhou *et al.* and more recently by Pershan (1994*a*), in the exact optical matrix calculation the non-linearity of the relation between reflectivity and structure as the critical angle is approached is able in principle to distinguish the different solutions in Fig. 2. The reason for this can be understood from Fig. 1 and (3) and (4). The reflectivity

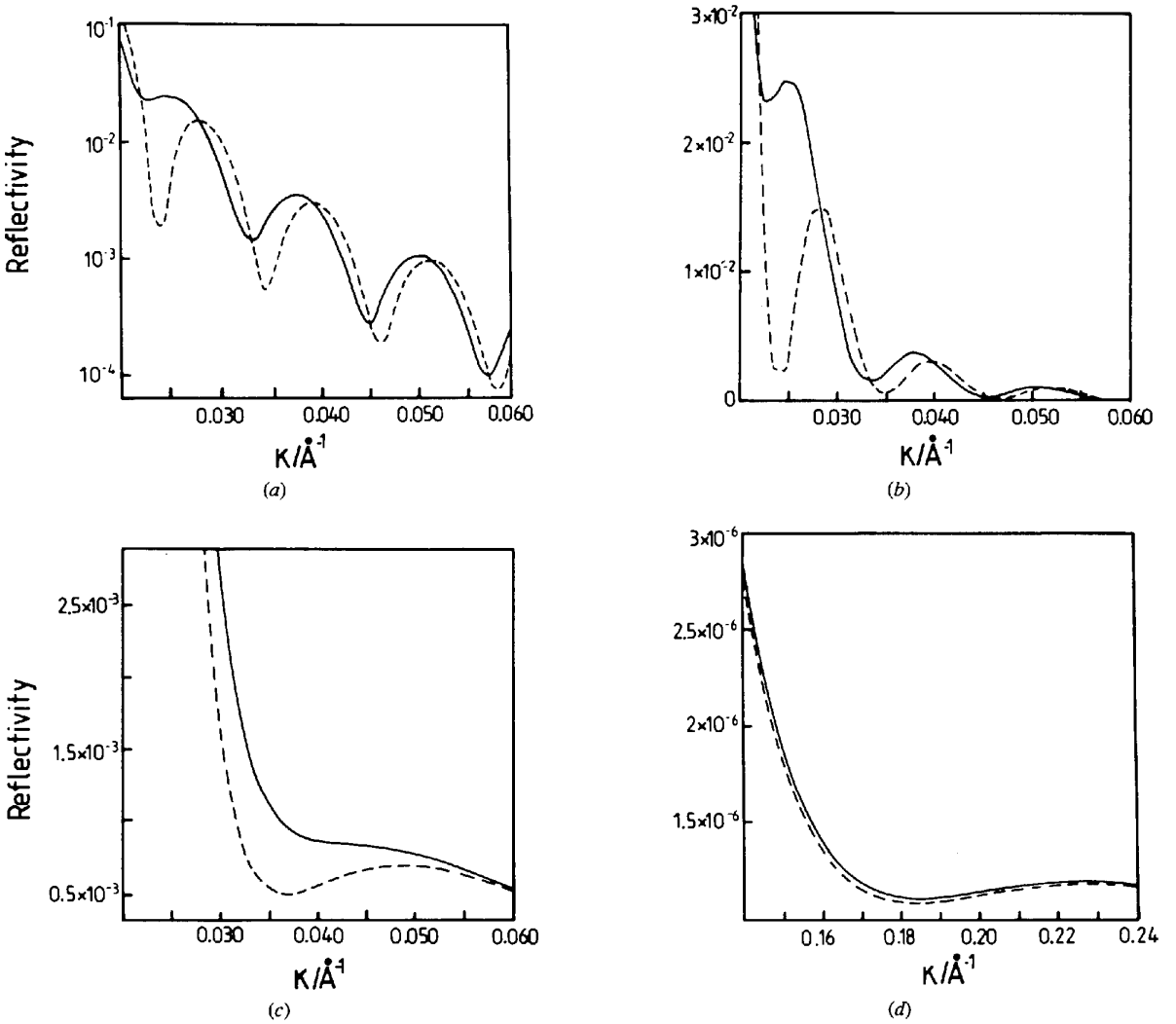

Fig. 3. Exact reflectivity profiles for the scattering-length-density profiles shown in Figs. 2(*a*) (dashed line) and (*b*) (solid line). The thickness of the monolayer is (*a*) and (*b*) 500 Å, (*c*) 100 Å and (*d*) 20 Å.

amplitudes at the first and second interfaces are quite different for the two situations shown in Figs. 2(*a*) and (*b*) and so is the phase shift β, and these differences become significant near the critical angle. The effect is shown in Fig. 3(*a*) for a layer 500 Å thick. On the logarithmic scale usually used for displaying reflectivity data, the differences can hardly be distinguished, but on a linear scale (Fig. 3*b*), there are clear differences, which ought to be measurable. Zhou & Chen (1993) have devised a fitting procedure that utilizes this non-linearity to solve the phase problem.

Most of the analysis of Zhou & Chen is concerned with the protocol for using information from different κ ranges to solve the phase problem. The inversion used is not a Fourier transform but a direct solution of the inverse equations of the optical matrix treatment. The authors show that the inversion is rigorous in two simple examples, but no such proof is possible in more complicated cases and the authors can only show that in a number of cases their inversion procedure does lead back to the original scattering-length-density profile. Whilst the basic claim of Zhou & Chen is mathematically correct, the method is only strictly applicable under particular conditions. We assume that the protocol of the calculation of Zhou & Chen is satisfactory and focus only on the experimental circumstances in which the non-linearity of the reflectivity leads to the phase, choosing the example shown in Fig. 2 and restricting ourselves for simplicity to the (*a*)/(*b*) pair. We take the two bulk phases to be air and D_2O and we consider the neutron reflectivity. The difference between the reflectivities of (*a*) and (*b*) is large when the thickness of the layer is 500 Å but, as can be seen in Figs. 3(*c*) and (*d*), becomes very small as the thickness decreases to 20 Å and would then often be obscured by experimental errors. It is difficult to draw a general conclusion but this result would suggest that the method of Zhou & Chen is not valid for a large number of commonly investigated systems where the dimensions are, say, less than about 50 Å. There are also occasions when it is not valid even when the dimensions are appropriate. The two structures of Figs. 2(*a*) and (*b*) are indistinguishable in the kinematic approximation but distinguishable in the optical matrix method when the thickness is large. It is possible, however, to modify one or other of the structures so that, although the two reflectivities never become mathematically identical, they can be made to be indistinguishable at the experimental level. Thus, Fig. 4 shows a pair of such structures and their corresponding reflectivities. The structural changes drawn in Fig. 4(*b*) could correspond to very small differences, in the vicinity of the surface, between the density of the substrate and its bulk value. It is not difficult to generate other small structural differences which cause the two basic profiles of Figs. 2(*a*) and (*b*) to give the same reflectivity within experimental error (see also Pershan, 1994*b*). In experiments on the solid/liquid interface, there are often contributions of just the type that would cause this ambiguity, for example, it is seldom possible to obtain zero reflectivity at perfect contrast match (McDermott, McCarney, Thomas & Rennie, 1994). This suggests that the whole method of Zhou & Chen, whilst correct in principle and useful on some occasions, must be used with caution.

The conclusion to be drawn from the above discussion is that there is usually a phase problem in practice. The most direct solution is then by means of an experiment that determines the phase and the amplitude. Fiedeldy, Lipperheide, Leeb & Sofianos (1992) have proposed that the phase could be determined from a measurement of the dwell time, but this seems far from being usable at present.

The procedure used by Pedersen (1992) and later extended by Hamley & Pedersen (1994) and Pedersen & Hamley (1994*a*, *b*) addresses both the phase problem

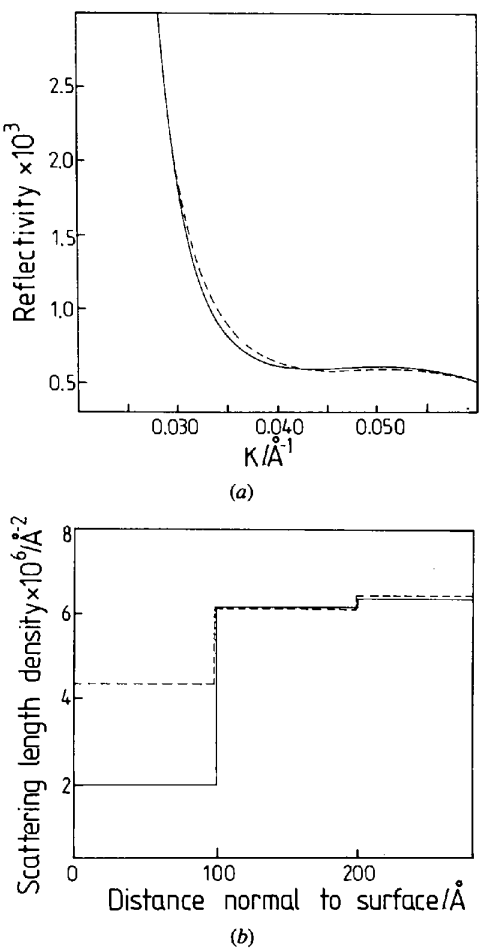

Fig. 4. Two scattering-length-density profiles that give the same reflectivity within typical experimental error. The modified versions of the scattering-length-density profiles in Figs. 2(*a*) and (*b*) are shown in (*b*) as dashed and solid lines.

and the difficulty of Fourier transforming reflectivities that have only been measured over a limited range of momentum transfer. In the sequence of data analysis, the latter comes first and we discuss it first. Glatter (1977) developed the method of the indirect Fourier transform (IFT) for inverting small-angle scattering data, in which, instead of doing the Fourier transform directly, the coefficients of the Fourier components of a suitably chosen basis set are determined by fitting them to the data. This avoids the distortion of the resulting Fourier transform by truncation errors. Pedersen has adapted this to the reflection experiment so that the IFT is applied to $P^{(1)}(\kappa)$ as obtained from (18) to obtain the Patterson of the derivative of the scattering-length-density profile, $P^{(1)}(z)$. Pedersen then assumes that the $P^{(1)}(z)$ profile will be a smooth function and shows that, for his purposes (mainly the analysis of insoluble monolayers on water), cubic B splines form more suitable basis functions than periodic functions. Pedersen has then adapted the same method of fitting the coefficients of the members of a basis set to do the square-root deconvolution of $P^{(1)}(z)$ to obtain $\rho^{(1)}(z)$. This is the stage at which the phase problem has to be solved. The justification of the procedure is based on the successful analysis of a number of test data but, unfortunately, examples where the solutions might be unstable, such as scattering-length-density profiles close to the profiles of Fig. 2, have not been tested and so it is difficult to judge the effectiveness of the method in terms of uniqueness. As admitted by Pedersen, it is also difficult to see that the method offers much advantage over direct fitting procedures. One important feature, however, is that the initial indirect Fourier transform ensures that the resolution of the experiment is included correctly. A limitation is that the method cannot at present be used for the simultaneous fitting of different reflectivity profiles from a given structure. Pedersen & Hamley have later extended the method to obtain $P^{(1)}(z)$ using basis functions of either cubic splines or periodic functions in conjunction with the exact optical matrix reflectivity.

Singh, Tirrell & Bates (1993) have independently developed the indirect Fourier transform technique to analyse reflectivity data from periodic structures. The method is essentially the same as that of Pedersen except that periodic (sine and cosine) functions are used as the basis set and, rather than obtaining the coefficients of all members of the basis set in one step, Singh *et al.* start by using the lowest Fourier components and progressively include higher terms. Although the kinematic approximation is used to determine the Fourier coefficients, they are refined at each stage by fitting the observed reflectivity exactly using the optical matrix calculation. As with the Pedersen method, the authors cannot prove that they have a unique solution but can only justify the method by its success in reproducing the correct structure from simulated data. However, the difference from Pedersen's work, which considers non-periodic structures, is that Singh *et al.* have found that their method is essential for the successful analysis of the multilayer systems that they are studying. This is because there are too many choices of model to be tested and the procedure of guessing a structure, comparing calculated and simulated profiles *etc.* is a hopeless task. The use of the indirect Fourier transform, especially in stepwise fashion, is effectively a means of making that choice rapidly and efficiently. This is greatly helped by the different effects of the sine and cosine terms in the basis set on the shapes of the Bragg peaks, which result from the combination of internal structure of the layer and its finite thickness. As the authors point out, they have no way of confirming the uniqueness of the structure rigorously but consistency of their determined structures with *a priori* knowledge of the sample gives strong support to the claim of uniqueness.

Sivia, Hamilton & Smith (1991) have suggested that a reference surface be included, which would be used to determine the phase. If the reference surface is perfectly sharp then

$$\rho^{(1)}(z) = \rho_0\delta(z-a) + \rho_s^{(1)}(z), \tag{31}$$

where a is the separation of the reference and the unknown interfacial scattering-length-density profile $\rho_s^{(1)}$ and

$$\rho^{(1)}(\kappa) = \rho_0 \exp(i\kappa a) + \rho_s^{(1)}(\kappa) \tag{32}$$

leading to

$$P^{(1)}(\kappa) = \rho_0^2 + |\rho_s^{(1)}(\kappa)|^2 + 2\Re\{\rho_s^{(1)}(\kappa)\rho_0 \exp(i\kappa a)\}. \tag{33}$$

The experiment determines $P^{(1)}(\kappa)$, which on Fourier transformation gives the Patterson function

$$P^{(1)}(z) = \rho_0^2\delta(0) + P_s^{(1)}(z) + \rho_0\rho_s^{(1)}(z-a). \tag{34}$$

This now contains phase information in the third term. The key to the analysis is that if a is chosen to be large the contribution of the third term is at large z and is easily separated from the main Patterson term $P_s^{(1)}(z)$. Thus, the phase information may be recovered and $P_s^{(1)}(z)$ deconvoluted to give $\rho_s^{(1)}$. There are obvious experimental difficulties and no such experiment has yet been performed. However, the equations above do show a path to the more straightforward use of isotopic substitution. We first apply them to another special case where the experiment has actually been carried out and where there is some possibility for applying the method more generally.

Penfold, Webster, Bucknall & Sivia (1994) deposited a polymer layer on a magnetic substrate (Ni) and then did two experiments with different polarization of the

magnetic substrate. The scattering length of an atom with a magnetic moment resulting from its electronic configuration contains components from the nucleus and from the magnetic moment associated with the electronic motion. Differently polarized atoms therefore have different scattering lengths and the scattering-length densities for nickel in its two magnetic states are also different [(ρ_+) and (ρ_-)]. If we neglect for the moment any inaccuracies in the kinematic approximation, the difference between the structure factors for the two magnetization states is, from (33),

$$P_+^{(1)} - P_-^{(1)} = \rho_+^2 - \rho_-^2 + 2(\rho_+ - \rho_-) \times \Re\{\rho_s^{(1)}(\kappa)\exp(i\kappa a)\}, \quad (35)$$

which on Fourier transformation gives

$$(\rho_+^2 - \rho_-^2)\delta(0) + (\rho_+ - \rho_-)\rho_s^{(1)}(z-a). \quad (36)$$

In practice, it is not necessary to restrict the solution using the kinematic approximation as above and the authors used the distorted wave Born approximation (Sanyal *et al.*, 1993) and successfully extracted $\rho_s^{(1)}(z-a)$.

The use of isotopic substitution, or the combination of X-ray and neutron reflectivities from the same system does not usually lead so directly to $\rho_s^{(1)}$. For simplicity, we assume that the scattering-length density can be written in terms of a sharp ρ_0, which is not affected by isotopic substitution, and a $\rho_s^{(1)}$, which scales with the scattering lengths of the isotopic species, *i.e.* $\rho_s^{(1)}(z) = b_a n^{(1)}(z)$. Then, using (33), we have two equations of the form

$$P_a^{(1)}(\kappa)/b_a^2 = \rho_0/b_a^2 + |n^{(1)}(\kappa)|^2 + (2/b_a)\Re\{n^{(1)}(\kappa)\rho_0\exp(i\kappa a)\}. \quad (37)$$

As ρ_0 is known, $|n^{(1)}(\kappa)|^2$ and $\Re\{n^{(1)}(\kappa)\rho_0\exp(i\kappa a)\}$ can be determined separately by solution of the two simultaneous equations and hence the phase information is recovered to give a unique structural profile. We also note that a similar experiment can be done with X-rays by working close to an X-ray absorption edge and using the anomalous scattering of a suitable atom (Sanyal *et al.*, 1993). In general, the simplifications made above are not always appropriate and, although having two profiles must improve the phase situation, model fitting may still be necessary to solve the structure, rather than direct inversion as in (36). The division of the reflectivity profile into partial structure factors, which we now describe, is generally a more satisfactory way of handling more than one reflectivity profile from a given structure.

Although we have emphasized the inherent ambiguity caused by the phase problem, it is often the case that simple assumptions about physically possible or probable structures or constraints imposed by other measurements are sufficient to ensure that the interpretation of the Patterson function, $P^{(1)}(z)$, to obtain a scattering-length-density profile is unique. On these occasions, direct Fourier transformation of $P^{(1)}(\kappa)$ may be the most satisfactory procedure if the range of momentum transfer is adequate (see, for example, Pershan, 1989; Schlossman *et al.*, 1991).

4. Partial structure factors

Most of the analyses of reflectivity data so far discussed are aimed at producing a unique solution for the scattering-length-density profile. We now focus on the more direct determination of the number density profiles of the different species through the interface. We first consider the limitations in the interpretation of a scattering-length-density profile.

In general, several species contribute to the scattering-length-density profile and the main purpose of the experiment is to determine the distribution of these individual species, *i.e.* (7) has to be solved for the number density profiles, $n_i(z)$. The simplest cases are those where either the scattering from all species other than the one of interest has been eliminated, *e.g.* by isotopic labelling in neutron reflection, or when one species dominates the scattering, *e.g.* a heavy ion in X-ray reflection, when $n_i(z) = \rho_i(z)/b_i$. In more complicated cases, there may be relations between the $n_i(z)$ that make it possible to solve (7). For example, if two of the components being examined are part of the same molecule, then stoichiometry requires that

$$\int n_1(z)\,dz = \int n_2(z)\,dz. \quad (38)$$

A second widely used constraint is often constructed by estimating the molar volume of two fragments constituting a layer and then assuming that the layer is close packed when

$$\int \overline{v_1} n_1(z)\,dz + \int \overline{v_2} n_2(z)\,dz = V. \quad (39)$$

These constraints are, however, difficult to use except with very simple model structures and the determination of a single scattering-length-density profile, no matter how accurate, may not be sufficient for the solution of (7). In many cases, this ambiguity may be more serious than any ambiguity arising from the loss of phase information or lack of resolution and yet it has been largely neglected. For a more detailed discussion of this point, the reader is referred to Lu & Thomas (1995).

The use of partial structure factors provides a basis for discussing the reflectivity in terms of the contributions from different components in the layer. Substituting (7)

into (18) gives

$$R = (16\pi^2/\kappa^4)\left[\sum_j b_j^2 h_{jj}^{(1)} + \sum_j \sum_{i<j} 2b_i b_j h_{ij}^{(1)}\right], \quad (40)$$

where the $h_{jj}^{(1)}$ are the *self* partial structure factors given by

$$h_{jj}^{(1)}(\kappa) = |n_j^{(1)}(\kappa)|^2 \quad (41)$$

and the $h_{ij}^{(1)}$ are the *cross* partial structure factors given by

$$h_{ij}^{(1)}(\kappa) = \Re\{n_i^{(1)}(\kappa) n_j^{(1)}(\kappa)\}. \quad (42)$$

The $n_j^{(1)}(\kappa)$ are the one-dimensional Fourier transforms of $n_j^{(1)}(z)$, the gradient of the average number density profile of group j in the direction normal to the surface, given by (20) but with n replacing ρ. Just as for the equations in ρ, there is a relation between $h^{(1)}(\kappa)$ and $h(\kappa)$:

$$\kappa^2 h(\kappa) = h^{(1)}(\kappa). \quad (43)$$

A self partial structure factor is thus related to the corresponding number-density profile in exactly the same way as the $P^{(1)}(\kappa)$ is related to the Patterson $P^{(1)}(z)$ and the problems of going from one to the other are amenable to the same methods of analysis. However, the cross partial structure factors defined by (42) offer new possibilities in the analysis. The shift theorem of Fourier transforms (Bracewell, 1978) states that if a one-dimensional distribution is moved by δ then its Fourier transform is changed by a phase factor, $\exp(i\kappa\delta)$, *i.e.* if

$$n_i'(z) = n_i(z - \delta), \quad (44)$$

then

$$n_i'(\kappa) = n_i(\kappa)\exp(i\kappa\delta). \quad (45)$$

Thus, (42) becomes

$$h_{ij}^{(1)}(\kappa) = \Re\{n_i^{(1)}(\kappa) n_j^{(1)}(\kappa)\exp(i\kappa\delta_{ij})\}, \quad (46)$$

where δ_{ij} is the separation of the two distributions. Important special cases occur when $n_j^{(1)}(\kappa)$ and/or $n_i^{(1)}(\kappa)$ are entirely real or imaginary. If they are both real or both imaginary, then

$$h_{ij}^{(1)}(\kappa) = n_i^{(1)}(\kappa) n_j^{(1)}(\kappa)\cos(\kappa\delta_{ij}), \quad (47)$$

and if one is real and the other imaginary,

$$h_{ij}^{(1)}(\kappa) = n_i^{(1)}(\kappa) n_j^{(1)}(\kappa)\sin(\kappa\delta_{ij}). \quad (48)$$

Equations (47) and (48) can be further simplified to obtain

$$h_{ij}^{(1)}(\kappa) = \pm[h_i^{(1)}(\kappa) h_j^{(1)}(\kappa)]^{1/2}\cos(\kappa\delta_{ij}) \quad (49)$$

and

$$h_{ij}^{(1)}(\kappa) = \pm[h_i^{(1)}(\kappa) h_j^{(1)}(\kappa)]^{1/2}\sin(\kappa\delta_{ij}), \quad (50)$$

where the $\pm$ arises from the uncertainty in the phase. The case of $n_j^{(1)}(\kappa)$ real corresponds to a distribution $n_j(z)$ that is symmetrical about its centre, *i.e.* an even function, and $n_j^{(1)}(\kappa)$ imaginary to an odd distribution. Many fragment distributions across interfaces approximate closely to these two limits and (49) and (50) then give a means of determining the separation between pairs of distributions *without* either doing the Fourier transform or making specific assumptions about the type of distribution (other than that they are even or odd). Equation (46) strictly holds only if there are no correlations in the plane of the interface, *i.e.* they must depend on no coordinate other than the single spatial coordinate, z. We discuss this question further in the section on roughness.

In what follows, we apply the partial-structure-factor method to a surfactant layer using a labelling scheme that divides the adsorbed molecular layer into nine fragments. The surfactant is hexadecyltrimethylammonium bromide [$C_{16}H_{33}N(CH_3)_3Br$, abbreviated to C_{16}TAB], which forms a monolayer at the air/water interface in equilibrium with bulk solution (Lu, Li, Smallwood, Thomas & Penfold, 1995). The surface concentration can be varied by changing the concentration of the bulk solution but here we consider only one surface concentration since our purpose is to examine the procedure of analysing the data. The resolution with which the structure of the adsorbed layer can be probed depends in part on the instrumental resolution and in part on the extent to which the layer can be broken down into identifiable labels. For C_{16}TAB, we have divided the layer into ten labelled species, the eight consecutive C_2H_4 fragments, the $N(CH_3)_3$ head group and the water. To illustrate the method, we start by considering the molecule as consisting of two labels, the C_{16} chain as a whole and the head. For this labelling scheme, the reflectivity can be written as

$$R = (16\pi^2/\kappa^4)[b_c^2 h_{cc}^{(1)} + b_h^2 h_{hh}^{(1)} + b_w^2 h_{ww}^{(1)} + 2b_c b_h h_{ch}^{(1)} + 2b_c b_w h_{cw}^{(1)} + 2b_h b_w h_{hw}^{(1)}], \quad (51)$$

where the subscripts c, h and w denote chains, heads and water, respectively. To determine the six partial structure factors in (51) requires six measurements of the reflectivity with different values of b_i. The most obvious combinations to choose in neutron reflectivity are the three measurements when each of b_c, b_h and b_w are respectively zero since this can easily be achieved by suitable hydrogen/deuterium substitution. When protonated, the heads have a scattering length almost exactly equal to zero. For typical hydrocarbon chains, it is necessary to mix H/D components in a molar ratio of about 10:1 and water also has a zero scattering length when it is about 10% heavy water (we refer to this as null reflecting water, abbreviated as NRW). Each

measurement with two of the b_i zero gives one self partial structure factor directly. The three cross partial structure factors are obtained by combination of these measurements with others where two or more b_i are non-zero. We discuss below how errors in the determination of the structure factors may be propagated by using contrast conditions that are not sufficiently distinct and we also discuss the problems of changes of the chemical structure associated with isotopic substitution. For the moment, we assume that neither of these presents any difficulty.

When the six partial structure factors are known, the three separations between them may be determined directly using (49) and (50) because, in dilute solution, both the head and chain distributions must be even to a first approximation and the water distribution is odd to a first approximation. The determination of these distances is shown in Fig. 5. Although there is an uncertainty in the sign in the application of the two equations, the constraint that

$$\delta_{cw} = \delta_{ch} + \delta_{hw} \qquad (52)$$

with the physical knowledge that the chain must be on the air side of the interface solves the phase problem for this particular structure. The values of the separations yield important structural information about the layer that has hitherto not been available and at a resolution of about 1 Å. This resolution is much higher than apparently possible from the usual criterion of π/κ_{max}, which is only about 10 Å for neutrons, although much higher, about 2.5 Å, for X-rays. We discuss this further below.

The complete analysis in terms of the six partial structure factors of (51) requires the fitting of the self partial structure factors. These have to be analysed either by Fourier transformation by one of the methods described above or by model fitting. However, because number-density distributions of fragments are a more natural way of describing structure across an interface than scattering-length-density profiles, it is usually easier to generate physically realistic models for the partial structure factors than for the Fourier transform of a complex scattering-length-density profile. We illustrate this for the C_{16}TAB layer, starting with the fitting using a multilayer model in conjunction with the optical matrix calculation.

The most successful *model* fitting of the scattering-length density of the C_{16}TAB and similar surfactant layers has so far been to use a two-uniform-layer model, the uppermost layer consisting of chains only and the lower layer of a mixture of head groups, water and a fraction of the hydrocarbon chains (Simister, Lee, Thomas & Penfold, 1992*b*). The constraint of close packing (39) is imposed on the lower layer, for which it is necessary to estimate the volumes of the components. The set of six isotopic data is best fitted with the structure shown in Fig. 6(*a*). It would be possible to introduce roughness at any of the three interfaces, and this would have some effect on the final parameters obtained for the layer, but the effect is small and, at the rather low resolution of the neutron experiment, is usually not worth doing. The situation is different in an X-ray reflection experiment where the resolution is much higher.

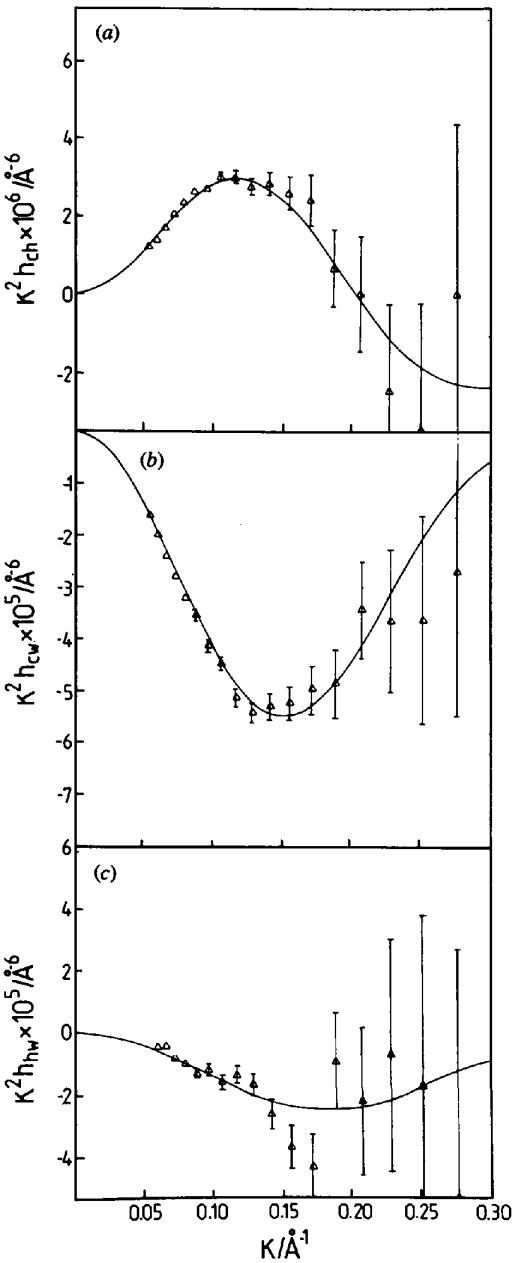

Fig. 5. The three cross partial structure factors of C_{16}TAB and the best fits (continuous lines) using equations (49) and (50) for (*a*) chain/head, (*b*) chain/water and (*c*) head/water. The separations of the respective distributions are δ_{ch} = 8.0 (5) Å, δ_{cw} = 9.0 (5) Å and δ_{hw} = 1 (1) Å.

In applying the partial-structure-factor method to this system, we first note that the number-density distributions of chains and heads will be approximately symmetrical distributions and the natural choices for their distributions are then a uniform layer, a uniform layer roughened on either side or a Gaussian. The dimensions of typical surfactant layers are such that, within the resolution of the neutron experiment, these models cannot be distinguished (Fig. 7). Although this means that there are limits to the accuracy of the description of the shapes of the distributions, the widths are accurately characterized. This is not necessarily the case where a more complex layer model has been fitted, when limitations in the description of the other components in the layer may affect the accuracy of the modelling of the fragment in question. We show the structures obtained from the best fits of the partial structure factors to uniform layers in Fig. 6(*b*) and to Gaussian distributions in Fig. 6(*c*). The water has been assumed to be a tanh distribution (25) for the latter and a step function for the former. Note that the determination of the separation between the distributions is not affected by the choice of uniform or Gaussian distributions, which is consistent with the analysis in terms of (49) and (50). We show below that the Gaussian distribution is more appropriate for these surfactant systems but it is interesting here to compare the three 'experimental' structures of Fig. 6 with a computer simulation of the same system shown as dashed lines in each of Figs. 6(*a*), (*b*) and (*c*) (Böcker, Schlenkrich, Bopp & Brickmann, 1992). The simulation is in remarkably good agreement with the structure shown in Fig. 6(*c*). The block structure of the surfactant layer is unsatisfactory either because, as in (*a*), it gives a somewhat unphysical distribution of the chains or because, in (*b*), it violates close-packing requirements in a narrow region. Either of these problems could be solved by using a finer subdivision of the layer or by the judicious use of roughness, but these introduce more fitting parameters. Division of the layer into its two structural units, head group and hydrocarbon chain, is the simplest description to use as a start.

It is particularly easy to make use of stoichiometric constraints in the fitting of partial structure factors. For example, for Gaussian and uniform layer-number distributions, the partial structure factors are, respectively,

$$h_{ii}^{(1)}(\kappa) = (\kappa^2/A^2)\exp(-\sigma^2\kappa^2/8) \quad (53)$$

$$h_{ii}^{(1)}(\kappa) = (4/A^2\tau^2)\sin^2(\kappa\tau/2), \quad (54)$$

where A is the area per molecule, which stoichiometry requires to be the same for each fragment in the layer. We will show below that, for these soluble surfactants, the correct distribution is a Gaussian and from now on we will not consider uniform-layer models.

The complete analysis of the structure of the C_{16}TAB layer using the partial-structure-factor method is then to fit the self partial structure factors with Gaussian distributions for the chain and head terms and a tanh profile for the solvent, and to fit the cross terms using the relatively model independent treatment based on (49) and (50) to obtain the δ_{ij}. There are two limitations of this procedure. Although there are only two independent δ_{ij} and therefore it is strictly necessary to determine only two of the cross terms in (51) and hence make only five measurements altogether, it is not in general possible to determine a chosen subset of cross partial structure factors without making all six measurements. It is a coincidence that it is possible with C_{16}TAB because the head scattering length can be made exactly zero, but it is not possible for molecules such as $C_{12}H_{25}(OC_2H_4)_mOH$,

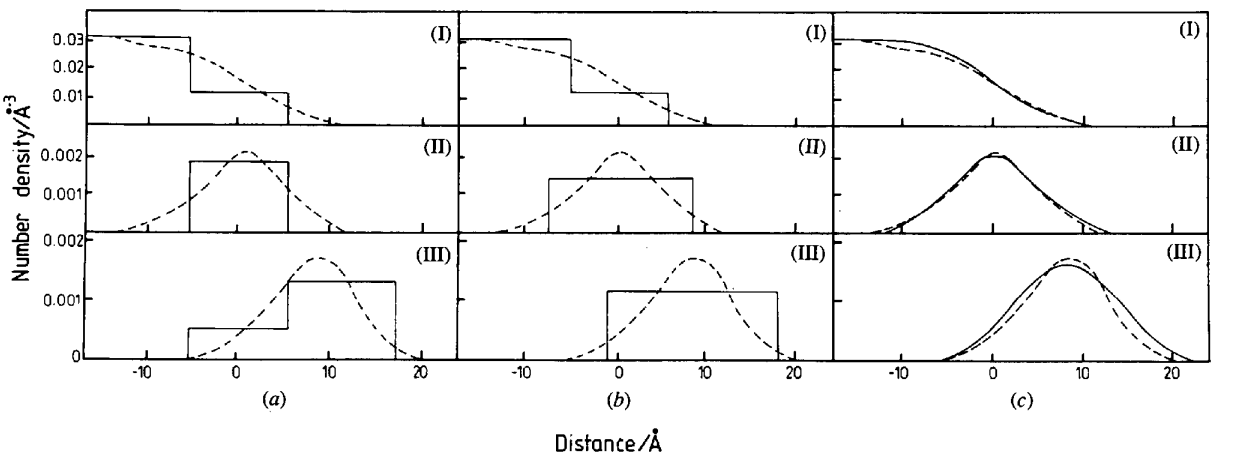

Fig. 6. Number-density distributions of chains, heads and water in the C_{16}TAB layer at its c.m.c. (area per molecule = 45 Å^2) from the best fits of (*a*) a two-uniform-layer model to the reflectivity, (*b*) single-block models to each of the partial structure factors, and (*c*) of Gaussian (head and chain) and tanh profiles (water) to the partial structure factors. The dashed lines are the same in each part of the diagram and are the number-density distributions obtained from a computer simulation on C_{16}TACl at the same area per molecule (Böcker, Schlenkrich, Bopp & Brickmann, 1992). The reference position has been chosen to be at the centre of the head distribution.

for example. The second limitation is that if one of the six data sets contains errors these will propagate through the solution of the simultaneous equations to give errors in one or more of the δ_{ij} and hence prevent a satisfactory analysis. The first of these problems can be solved, and the second minimized, by using partial structure factors to describe the reflectivity, but then to fit the set of reflectivities directly using the δ_{ij} as adjustable parameters, together with the parameters required to describe the width and shape of the self partial structure factors. This is the basis of the method used by Lee & Milnes (1995), which we now describe.

The reflectivity is given by (51) with six independent adjustable parameters, σ_c, σ_h, ζ_w, δ_{ch}, δ_{cw} and A, the area per molecule, and becomes analytic if we assume the number distributions to be Gaussians for the chains and heads, and a tanh profile for the water. Instead of determining each of these parameters separately after solving (51) for the partial structure factors, we do a non-linear least-squares fit of the six unknown parameters to the whole set of reflectivities, minimizing the quantity $F(i,\kappa)^2$, where

$$F(i,\kappa) = \sum_i \sum_\kappa [\log R_{\rm obs}(i,\kappa) - \log R_{\rm calc}(i,\kappa)]. \quad (55)$$

The standard errors in the fitting procedure are the square root of the variances of the regression coefficients and the variances are estimated numerically from the Jacobean matrix at the solution. We extend the lower range of κ for which the fitting may be done by using (30) to modify the kinematic reflectivity. The validity of the use of (30) near the critical angle depends on the dimensions of the layers being studied. For surfactant layers at the air/water interface, all the structure factors are either close to zero or, in the case of the water, approximately constant in the region of κ_c. In these circumstances, a relatively low accuracy is required in any formula for the correction of the kinematic reflectivity and therefore the calculation of the reflectivity is essentially exact.

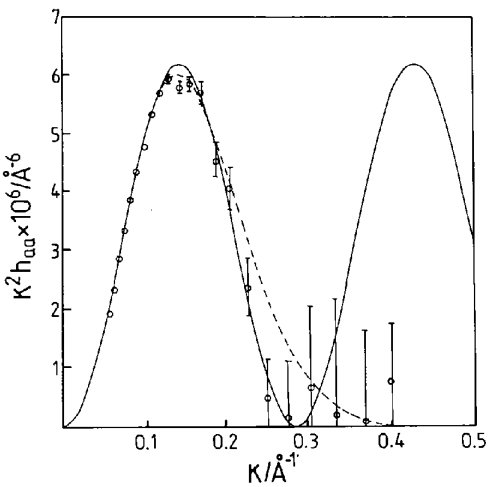

Fig. 7. Failure to distinguish between a Gaussian (dashed line) and a uniform layer (continuous line) for a monolayer of $C_{12}E_3$ (points) adsorbed at the air/liquid interface.

Each error determined from the Jacobean is a measure of the width of the overall minimum with respect to each of the minimized parameters and gives a useful guide as to how well the data determine a given parameter. The true error would also contain the error arising from the statistical quality of the data, which we have not included. Thus, the errors quoted in the tables below are only those appropriate to perfectly determined reflectivity profiles. In fitting a single reflectivity profile by least squares, it is usual practice to include the statistical errors at each measured point. However, as we have mentioned earlier, there are several factors that make the statistical errors much less dominant and more difficult to quantify as the number of data sets increases. The problem arises from systematic errors in the reflectivity profiles, arising from calibration error, sample contamination, small isotopic effects, inaccurate determination of isotopic composition and inaccurate background subtraction, some of which are discussed further below. The statistical errors in a profile vary enormously because of the rapid decay of the reflectivity with momentum transfer and become insignificant at low κ. The situation is further complicated because the reflectivity at low κ when the solvent is D_2O is much higher than when it is NRW, and therefore has a very low statistical error, but it is almost completely insensitive to the structure of the layer at the dimensions being considered here. If there were no systematic errors, this would not present any difficulty and the statistical errors could be included to give the true error. However, in the situation described, the inclusion of the statistical weighting, by giving undue weight to the low-κ data, may prevent a sufficiently rigorous fit to the high-κ data, which contain the important structural information. The quoted errors are therefore underestimates of the true error but give a good guide to their likely magnitude.

The results of such a fit to the C_{16}TAB data are compared with the results of fitting the individual partial structure factors in Table 1 (Lee & Milnes, 1995). The agreement between the two methods when the same set of six different reflectivity profiles are fitted is within the quoted error except for the width of the head-group distribution, where there is a significant discrepancy. As will be shown below, the width of the head group can be determined independently by a completely different experiment and is 14.0 (5) Å, whereas the least-squares fitting gives 17.8 (5) Å. The discrepancy was found to result partly from one poor set of data and partly because it is the parameter least well defined by the experiment. We discuss this further below.

Table 1. *Structural parameters of a C_{16}TAB layer determined by two methods (Å)*

	A (Å^2)	σ_c (Å)	σ_h (Å)	ζ (Å)	δ_{ch} (Å)	δ_{cs} (Å)	δ_{hs} (Å)
Partial structure factor	43.0 (10)	16.5 (20)	14.0 (30)	6.0 (10)	8.0 (5)	9.0 (5)	2 (1.5)
Least squares	44.5	16.6 (3)	17.8 (5)	7.6 (2)	8.7 (8)	9.3 (2)	0.6 (6)

Table 2. *Structural parameters of a C_{16}TAB layer determined by least-squares fitting using different data sets*

Data sets used	σ_c (Å)	σ_h (Å)	ζ (Å)	δ_{cs} (Å)	δ_{hs} (Å)	$\langle F(i,q)\rangle \times 10^3$
A, B, C, D, E, F	16.6	17.8	7.6	9.3	0.6	5.7
B, C, D, E, F	16.6	17.8	7.6	9.3	0.6	6.3
A, C, D, E, F	16.3	16.1	7.4	9.5	0.0	6.3
A, B, D, E, F	16.2	26.4	7.4	9.3	1.4	4.2
A, B, C, E, F	16.7	17.5	7.5	10.2	1.6	5.2
A, B, C, D, F	16.5	17.5	7.7	8.6	1.8	3.7
A, B, C, D, E	15.9	17.8	6.7	9.4	0.6	5.2
A, B, C, D, X	18.0	14.0	8.0	9.4	1.4	3.7

The labels refer to the data sets (*A*) dC$_{16}h$TAB in NRW, (*B*) dC$_{16}d$TAB/NRW, (*C*) '0'C$_{16}d$TAB/NRW, (*D*) dC$_{16}h$TAB/D$_2$O, (*E*) dC$_{16}d$TAB/D$_2$O, (*F*) hC$_{16}d$TAB/D$_2$O, where NRW refers to null reflecting water and '0' means that the H/D ratio in the hydrocarbon layer is such that it is also null reflecting. *X* is the X-ray reflectivity from hC$_{16}h$TAB/H$_2$O.

When the whole set of data is fitted it is no longer necessary to make the six isotopic substitutions to obtain the six partial structure factors. All that is needed is that enough data are available to determine the set of unknown parameters. The discussion of (52) showed that at least one of the six reflectivity profiles was not needed but, given that each partial structure factor contributes at different levels as κ varies, it is possible that fewer than five might determine the structure adequately. Which ones is not easy to decide without prior knowledge of the structure. In Table 2, we give the results of fitting sets of reflectivity profiles less than the six by least squares. Interestingly, any five of the six profiles give a set of parameters similar to those from the six, except for the set where the profile with only the head group deuterated is omitted (*C*), when the fitted value of the head-group width is hopelessly wrong. This is the measurement that is normally used to give σ_h directly. Of special interest is the possibility of including X-ray reflectivity data in the fitting scheme. Several authors have used parallel fitting of models to the neutron and X-ray profiles from the same system to determine the interfacial structure (Styrkas, Thomas, Adib, Davis, Hodge & Liu, 1994; Vaknin, Als-Nielsen, Peipenstock & Losche, 1991) but do not seem to have used a single minimizing routine. The larger κ range of the X-ray profile presents no difficulty when the reflectivity is expressed in terms of partial structure factors. The last set of fitted parameters in Table 2 includes five of the neutron reflectivities and the X-ray data. This is not such a consistent fit and it is clear that the X-rays are introducing a little confusion into the distinction between chain and head groups. This is exactly as one would expect since the region near the chain/head boundary is only slightly contrasted with the water for the X-rays, and the bromide counterions also make a significant contribution to the X-ray reflectivity, which has not been separated from that of the head group. The simultaneous fitting of X-ray and neutron data will, in general, be of considerable value because there may be many occasions where significant isotope effects on the structure preclude the use of isotopic data. Since it is always possible to obtain both neutron and X-ray reflectivity profiles, and it does not matter which isotopic species is chosen, it is interesting to try to assess the optimum choice for surfactant layers. For this purpose, we have chosen a surfactant where there is no contribution from counterions, the non-ionic surfactant $C_{12}H_{25}(OC_2H_4)_3OH$ (abbreviated to $C_{12}E_3$).

The structure of $C_{12}E_3$ has been determined with the same subdivisions as C_{16}TAB above using six isotopic measurements to obtain the relevant six partial structure factors (Lu, Hromadova & Thomas, 1993; Lu, Lee, Thomas, Penfold & Flitsch, 1993; Lu, Simister, Lee, Thomas, Rennie & Penfold, 1992). In addition, we have measured the X-ray specular reflectivity in the laboratory (Styrkas, 1994). We have observed no isotope effects in the surface tension of $C_{12}E_3$ solutions and, possibly because it is non-ionic, we have found it not only a particularly reproducible system but the surface excess determined from the Gibbs equation and surface tension agrees exactly with that determined by neutron reflection. Thus, the general level of accuracy of these measurements and their interpretation is higher than for C_{16}TAB. To be set against this, the contrast between hydrocarbon chains, ethoxy chains and water is very poor for X-rays and therefore it is impossible, for example, to obtain the surface excess accurately from X-ray reflection.

The results of non-linear least-squares fitting to the six neutron data sets and to the six neutron data sets with X-ray reflectivity are compared in rows 2 and 3 of Table

Table 3. *Parameters of a $C_{12}E_3$ layer determined by fitting different data sets*

Data set	A (Å^2)	σ_c (Å)	σ_e (Å)	ζ (Å)	δ_{cw} (Å)	δ_{ew} (Å)
Partial structure factor	36 (1)	16.5 (10)	15.5 (10)	6.0 (10)	10.0 (5)	2.5 (10)
A, B, C, D, E, F	35.8 (4)	16.6 (2)	17.3 (3)	6.0 (1)	10.3 (1)	2.6 (3)
A, B, C, D, E, F, X	36.0 (7)	16.3 (2)	17.4 (4)	5.8 (2)	10.2 (2)	2.8 (4)
D, surface tension	36	15.5 (5)	20.5 (38)	5.5 (5)	9.7 (5)	0.8 (11)
X, surface tension	36	16.1 (107)	24.0 (245)	4.7 (17)	7.1 (48)	7.0 (108)
D, X	45.1 (76)	13.1 (17)	14.6 (14)	6.6 (13)	9.2 (8)	0.7 (16)
D, X, surface tension	36	15.7 (4)	16.5 (10)	5.4 (5)	10.0 (2)	2.6 (6)
A, X	35.9 (15)	17.9 (7)	11.1 (22)	1.9 (12)	10.1 (8)	4.9 (16)

The labels refer to the data sets (*A*) $d\mathrm{C}_{12}h\mathrm{E}_3$ in NRW, (*B*) $d\mathrm{C}_{12}d\mathrm{E}_3$/NRW, (*C*) $h\mathrm{C}_{12}d\mathrm{E}_3$/NRW, (*D*) $d\mathrm{C}_{12}h\mathrm{E}_3/\mathrm{D}_2\mathrm{O}$, (*E*) $d\mathrm{C}_{12}d\mathrm{E}_3/\mathrm{D}_2\mathrm{O}$, (*F*) $h\mathrm{C}_{12}d\mathrm{E}_3/\mathrm{D}_2\mathrm{O}$, where NRW refers to null reflecting water. *X* is the X-ray measurement on $h\mathrm{C}_{12}h\mathrm{E}_3/\mathrm{H}_2\mathrm{O}$. The partial-structure-factor method fits the individual partial structure factors obtained directly from the reflectivity, the remainder have been fitted to the whole set of reflectivities by least squares.

3, the analysis in terms of the partial structure factors being given in row 1. The agreement is good, apart again from the head-group width, and the introduction of the extra X-ray set of data makes little difference to the final parameters. The question now arises as to which would be the best isotopic species to study on its own, *i.e.* by surface tension, X-ray and a single neutron reflection measurement. Since we know that there are no significant isotope effects in this system, we assume for what follows that the X-ray reflectivity is the same for all isotopic compositions. In a situation where isotope effects were expected, the correct X-ray measurement would have to be made. The most sensitive single measurement for obtaining the structure from a neutron reflection experiment should be $d\mathrm{C}_{12}h\mathrm{E}_3/\mathrm{D}_2\mathrm{O}$ (designated *D* in Table 3) because there is good contrast between the outer deuterated chain layer, the middle partially deuterated layer (ethylene glycol and $\mathrm{D}_2\mathrm{O}$) and the $\mathrm{D}_2\mathrm{O}$. However, such a measurement could not give an accurate model-independent value of the surface excess. Taking this measurement alone with the known surface excess gives the set of parameters in row 4 of Table 3. The large error in σ_e indicates that this quantity is completely unreliable, as indicated by its value, and related to this is the obviously incorrect value of δ_{ew}. However, the chain width, solvent width and chain–solvent distance are accurately determined by the single reflectivity measurement with the known surface area. Not surprisingly, the X-ray reflectivity, which is not very different from that of pure water, does not really determine any of the parameters successfully (row 5) as manifested by the large standard errors throughout. Combining the two data sets *D* and *X* without constraining the surface area also fails (row 6) but the combination of *D*, *X* and the known surface area gives a set of structural parameters within error the same as obtained from the full set (row 7). This is clearly a case where the choice of the right isotopic species for the single neutron measurement can be used in conjunction with a not very promising X-ray profile and surface-tension data to give a complete account of the structure. The correponding fits to the reflectivity data are shown in Fig. 8. Another combination that might be thought effective is $d\mathrm{C}_{12}h\mathrm{E}_3$/NRW (*A*) with the X-ray profile. This is because the X-ray reflectivity is most sensitive to the thickness of the region lying above the water, because it has a lower scattering-length density, and to the cross term between this layer and the 'solution' plane. The neutron profile depends only on the thickness of the hydrocarbon-chain region and gives an accurate value of the surface excess without recourse to surface-tension measurements. The results from just *A* and the X-ray profile are given in the final row of Table 3. Whilst the results are not as good as those from the other binary combination because the experiment fails to distinguish water and ethoxy chains clearly, they nevertheless show that the combined techniques *on the right isotopic species* could be very powerful in less unfavourable situations.

We now return to the C_{16}TAB layer and attempt to reach a division of the layer sufficiently fine that the assumed shapes of each fragment distribution reach a well defined limit. Experimentally, all interfaces have some roughness and the shape of the distribution of an infinitesimal element of the layer is entirely determined by the function that describes the roughness, which is expected to be a Gaussian. This is the same argument as made by Denton, Gray & Sullivan (1994). Thus, if the isotopic labelling of the layer were sufficiently fine, the structure of the layer would be exactly defined by the similar Gaussian distribution of all the fragments and the set of values of the separations of the fragments. It is interesting to explore the level of subdivision necessary to achieve this for the C_{16}TAB layer. Approximately, the width, σ_i, of the distribution of any fragment is given by

$$\sigma_i^2 = l_i^2 + w^2, \tag{56}$$

where l_i is the intrinsic structural width of the fragment and w is the roughness. This equation assumes both distributions are Gaussian. The value of l_i will be a function of the length of the label. For example, if it

increases linearly with the number of C atoms, n, in the hydrocarbon chain, (56) becomes

$$\sigma_i^2 = (nl)_i^2 + w^2. \quad (57)$$

The assumption that the distribution is always Gaussian may breakdown when the length of the fragment becomes sufficiently large. However, (57) is only being used to obtain an empirical extrapolation to small n, for which it should be sufficiently accurate. Fig. 9 shows a plot of σ_i^2 against n^2 for C_{16}TAB, where the head group (counting as one atom) is always deuterated and the length of the labelled carbon chain is increased in steps of two atoms at a time. Although the plot is not linear over the whole length of the chain, it gives a good extrapolation to a roughness of 14.0 (5) Å, defined in terms of the width of a Gaussian at $1/e$ of its height [see (24)]. The measurements show that the width of any fragment less than about three C atoms is approximately determined only by the roughness of the layer. Thus, from the argument above an accurate determination of the layer structure can be made from a subdivision of the surfactant layer into elements of three C atoms or less. The limits on such an experiment are that the reflectivity depends on the square of the unit size and it may become too small to measure against the incoherent background. The errors in δ_{ij} also become large at small separations. In the set of experiments we review here, we attempt to assess those limits.

We use two labelling schemes with the hydrocarbon chain divided into labelled C_4 or C_2 units, respectively (Lu, Li, Smallwood, Thomas & Penfold, 1995). In each case, the labelled unit is combined in a single compound either with a deuterated head group, in which case we determine δ_{nh}, or combined with labelled solvent, in which case we determine δ_{nw}, where n denotes the labelled fragment. In addition, we have made the combinations of pairs of labelled C_4 units such that we also determine δ_{mn} where m and n are two different labelled units. For the example of the combination of single C_4 and head-group labels, the reflectivity is given by

$$R = (16\pi^2/\kappa^4)[b_n^2 h_{nn}^{(1)} + b_h^2 h_{hh}^{(1)} + 2b_n b_h h_{nh}^{(1)}] \quad (58)$$

and three measurements suffice to determine the structure in terms of the two widths and the one separation. For this system, it is possible to choose either b_n or b_h to be exactly zero so that $h_{nn}^{(1)}$ and $h_{hh}^{(1)}$ are determined directly in a single measurement. The level of the signal from the head group or a C_4 group on its own is sufficient to obtain the width of the distribution but not with very great accuracy. It is not possible at all to do the experiment on a single C_2 group. However, the analysis of (58) is still possible because the width of the C_2 and C_4 distributions are determined by the roughness of the layer and, given that the surface coverage is identical for all the measurements, $h_{jj}^{(1)}$ is then identical for the head group, all C_2 groups and all the C_4 groups. This is

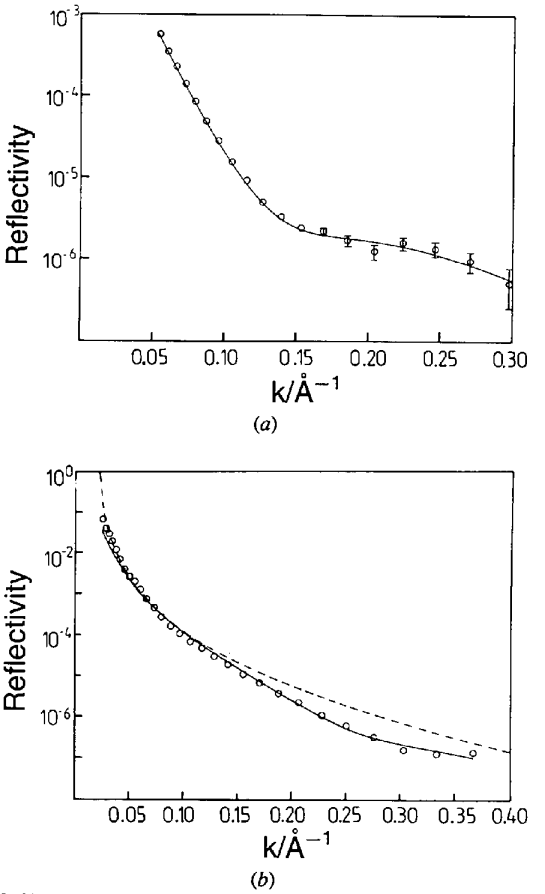

Fig. 8. Simultaneous least-squares fitting of neutron and X-ray reflectivity data for a monolayer of $C_{12}E_3$ adsorbed at the air/water interface. The neutron data (*a*) is for the isotopic species $dC_{12}hE_3$ in D_2O. In the plot of the X-ray data (*b*), the reflectivity from clean water is shown as a dashed line. The fitting parameters are those from the row labelled *D, X*, surface tension in Table 3.

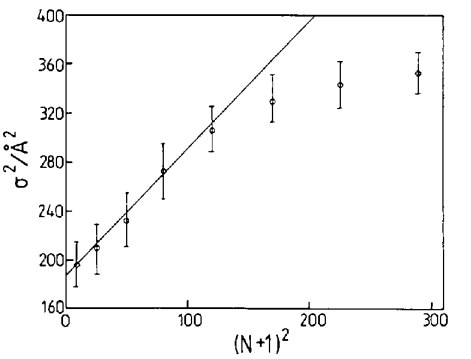

Fig. 9. The plot of the square of the thickness (σ^2) *versus* the square of the chain length $(N + 1)^2$, expressed in terms of the number of C atoms, N, for a monolayer of C_{16}TAB adsorbed at the air/water interface. The intercept gives the square of the roughness of the layer, 14 (1) Å. The slope is related to the projection of the chain along the normal direction.

Table 4. *Parameters of a C_{16}TAB layer from the partial structure factors*

	(*a*) (E.s.d. 1 Å)	(*b*)		(*a*) (E.s.d. 0.8 Å)	(*b*)
$\delta_{4h}(1)$	2.5	2.5	$\delta_{4w}(1)$	2.7	3.2
$\delta_{4h}(2)$	7.5	6.5	$\delta_{4w}(2)$	7.2	7.2
$\delta_{4h}(3)$	9.5	8.9	$\delta_{4w}(3)$	10.2	9.6
$\delta_{4h}(4)$	12.0	11.8	$\delta_{4w}(4)$	12.5	12.5
$\delta_{44}(1\text{–}2)$	4.0	4.0			
$\delta_{44}(1\text{–}3)$	7.5	6.4			
$\delta_{44}(1\text{–}4)$	10.5	9.3			
$\delta_{44}(3\text{–}4)$	2.0	2.9			
	(*a*) (E.s.d. 2 Å)	(*b*)		(*a*) (E.s.d. 2 Å)	(*b*)
$\delta_{2h}(1)$	1	1.3	$\delta_{2w}(1)$	2.5	2.0
$\delta_{2h}(2)$	4	3.6	$\delta_{2w}(2)$	4	4.3
$\delta_{2h}(3)$	5	5.5	$\delta_{2w}(3)$	6	6.2
$\delta_{2h}(4)$	6	7.4	$\delta_{2w}(4)$	7.5	8.1
$\delta_{2h}(5)$	7	8.4	$\delta_{2w}(5)$	8	9.1
$\delta_{2h}(6)$	8	9.3	$\delta_{2w}(6)$	9	10.0
$\delta_{2h}(7)$	11	11.2	$\delta_{2w}(7)$	11.5	11.9
$\delta_{2h}(8)$	12	12.4	$\delta_{2w}(8)$	13	13.1
δ_{2h}(inner)	4.0 (10)	3.7	δ_{6w}	5.5	4.4
δ_{ch}	8.5 (10)	8.0	δ_{cw}	9	8.7
δ_{hw}	2	0.7			
δ_{88}	6	5.4	δ_{8h}	5.5 (10)	4.7
δ_{2h}(outer)	12 (1)	11.9			

The labelling of the fragment is (1), (2) *etc.*, where (1) is the group nearest the head group. (*a*) refers to the values directly determined from the partial structure factors, (*b*) are the values obtained from a least-squares fit of the nine independent structural parameters to the whole set of data.

indicated by the results of Fig. 9 and confirmed by direct measurement. In these circumstances, the reflectivity is given by

$$R = (16\pi^2/\kappa^4)[(b_n^2 + b_h^2)h_{hh}^{(1)} + 2b_n b_h h_{nh}^{(1)}] \qquad (59)$$

and $h_{nh}^{(1)}$ can be further simplified to

$$h_{nh}^{(1)} = \pm h_{hh}^{(1)} \cos \kappa\delta_{nh}. \qquad (60)$$

In principle, once the $h_{hh}^{(1)}$ profile has been determined only a single measurement with the two deuterated labels in place is necessary to determine the appropriate δ_{nh} value. In practice, much improved statistics are obtained by obtaining an average $h_{hh}^{(1)}$ by summing over the independently determined profiles of the C_4 and head-group fragments or, better still, by taking $h_{hh}^{(1)}$ to be determined by a Gaussian distribution with the extrapolated width from Fig. 9. From the determination of the appropriate reflectivity profiles, the values of the various δ_{nh}, δ_{nn} and δ_{nw} given in Table 4 were determined. Given that the structure can be defined in terms of only nine independent separations, this represents a considerable overdetermination of the structure. To obtain a final set of parameters, the set in Table 4 were fitted by least squares to give the global set of nine parameters in Table 5. The results in Table 5 have been divided into two groups, those obtained only from the C_4 fragments, which lead to only five independent separations, and those from the C_2, which lead to nine. An example of the fitted results is given in Fig. 10 for the cross partial structure factors between the different C_4 fragments and the head group. These demonstrate the sensitivity of the reflectivity to the relative position of the C_4 fragment and head group. Examination of the partial structure factors involving the C_2 fragments showed them to be of rather poor statistical quality and therefore the δ_{2h} and δ_{2w} are much less accurate than the corresponding δ_{4n} quantities.

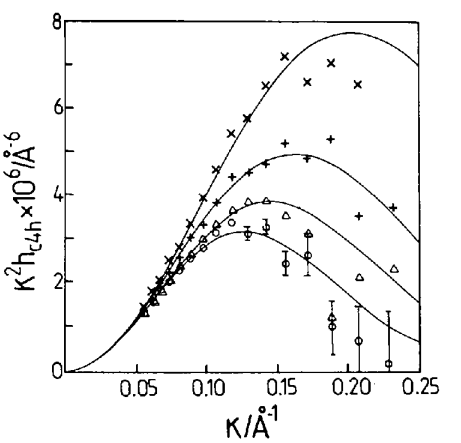

Fig. 10. The cross partial structure factors between different C_4 fragments and the head group for a monolayer of C_{16}TAB adsorbed at the air/water interface. The four structure factors have been fitted with equation (49) using Gaussians of width 14 Å for the chain fragment and head distributions and values of $\delta_{4h}(n)$ of × 2.5, + 7.5, △ 9.5 and o 12 (1) Å for n = 1, 2, 3 and 4, respectively. The value of n denotes the position of the C_4 group, 1 being nearest the head group. Error bars are only shown for n = 4 for clarity.

Table 5. *Parameters of a C_{16}TAB layer determined by direct fitting of the reflectivity and by least-squares fitting of the parameters in Table 4 (values in Å unless otherwise stated)*

(*a*) C_2 fragments labelled

Label	Reflectivity	Partial structure factor
σ_{c2}	13.8 (5)	14 (0.5)
σ_h	13.7 (5)	14 (0.5)
ζ	6.9 (2)	6.0 (10)
$\delta_{2w}(8)$	13.4 (6)	12.4 (10)
$\delta_{2w}(7)$	12.1 (7)	11.2 (10)
$\delta_{2w}(6)$	10.2 (8)	9.3 (10)
$\delta_{2w}(5)$	10.0 (7)	8.4 (10)
$\delta_{2w}(4)$	7.8 (7)	7.4 (10)
$\delta_{2w}(3)$	7.0 (8)	5.5 (10)
$\delta_{2w}(2)$	4.1 (10)	3.6 (10)
$\delta_{2w}(1)$	2.3 (10)	1.3 (10)
δ_{hw}	0.3 (1)	0.7 (5)
A (Å^2)	44.9 (7)	45 (1)

(*b*) C_4 fragments labelled

Label	Reflectivity (*a*)	Reflectivity (*b*)	Partial structure factors
σ_{c4}	12.0 (5)	14	14 (5).51
σ_h	9.8 (5)	14	14 (5)
ζ	6.0 (2)	6.2 (2)	6.0 (10)
$\delta_{4w}(4)$	13.0 (3)	12.7 (3)	12.4 (5)
$\delta_{4w}(3)$	11.1 (2)	10.5 (2)	10.0 (5)
$\delta_{4w}(2)$	8.5 (3)	7.6 (3)	7.0 (5)
$\delta_{4w}(1)$	3.8 (3)	3.3 (3)	2.6 (10)
δ_{hw}	0.1 (2)	0.2 (2)	0.2 (5)
A (Å^2)	46.4 (7)	43.0 (5)	45 (1)

The reflectivity (*b*) fits are obtained with the constraint that the thickness of the C_4 unit and the head group is 14Å. The labelling of the fragment is (1), (2) *etc.*, where (1) is the group nearest the head group.

This shows that at the signal levels presently available in neutron reflectometers the resolution is limited to groups containing about four C atoms, although it should be noted that the situation is sensitive to the coverage.

It is clear that in the determination of the δ_{ij} directly from the individual partial structure factors more weight is given to some profiles than to others. Thus, the average $h_{hh}^{(1)}$ profile is used in a large number of the determinations. It might be thought preferable to give equal weight to each reflectivity profile and this can be achieved using the least-squares fitting of the nine independent separations, the single value of the width of a small fragment, the area per molecule and the width of the solvent distribution, ζ, to the complete set of reflectivity profiles. The results of this simultaneous fitting to 45 reflectivity profiles are also given in Table 5 and the agreement between the two procedures is seen to be excellent. As would be expected from fitting such a large set of data, it is very easy to be trapped in false minima and it is necessary to impose a number of constraints to ensure rapid progress towards a global minimum. Particular difficulty was introduced by the C_2 fragments because the accuracy of the data and the resolution of the experiment was such that the separation of adjacent units was somewhat uncertain. The first constraint to circumvent this problem was to make the restriction that each successive C_2 unit in the lower part of the layer (nearest the water) was further from the water than the preceding group, *i.e.* there is no back-folding in the lower eight C atoms. The second constraint was that the distance between adjacent C_2 units could not exceed the known bond distances in the fully extended molecule. Finally, a restriction was put on the packing at any point in the layer, that it could not exceed a volume fraction 10% more than unity. This has no effect on the dimensions of the chain, but is found to have a slight effect on the position of the solvent dividing plane. For the technical details of how the volume packing constraint is introduced, the reader is referred to Lee & Milnes (1995).

The results of the least-squares fitting to the 45 reflectivity profiles is summarized by the parameters for the C_2 fragments in Table 5(*a*) and for the smaller number of profiles appropriate to the division into C_4 units in Table 5(*b*). The agreement between the fitting of each partial structure factor and of the whole set of reflectivities in Table 5(*a*) is within error, although the least-squares results give systematically larger values of δ_{nh}. This may be a coincidence given the large errors. In Table 5(*b*), the least-squares fitting in column 1 [reflectivity (*a*)] gives systematically larger values of the δ_{nh} and two σ values that are much too low. Since both σ values are known independently, and accurately, from the plot of Fig. 9, we have repeated the fitting with both

σ constrained to 14 Å, to obtain the set of parameters in column 2 [reflectivity (*b*)]. The agreement with the values determined from the partial structure factors is now very much better. It should be emphasized that we are not necessarily seeking good agreement; the purpose being to devise as objective as possible a procedure for fitting the data, but one that takes fully into account the strengths and weaknesses of the experiment. The use of these constraints will be further discussed under *Resolution and systematic errors* below. Finally, we show the least-squares fits to the set of reflectivities from '0'$C_{4m}dC_4$'0'$C_{12-4m}h$TAB in D_2O, where '0' indicates a scattering length of zero. These are dominated by the separation of the labelled C_4 group and the mid-point of the D_2O distribution ('the solvent plane'). As for the partial structure factors in Fig. 10, the reflectivity can be seen to be very sensitive to the position of the C_4 group, the interference becoming more pronounced as the separation increases.

Given that we have assumed a Gaussian distribution for the chain as a whole both in fitting to the self partial structure factors and in using (49) and (50), it is interesting to assess that assumption. The distribution of the chain as a single unit can be determined by building it up from the distribution of smaller fragments and their known separations. This can be approached in several ways. Although the limiting shape of the distribution of a small fragment is almost certainly Gaussian, it is not necessary to assume this. It could be taken to be a uniform layer and this makes no significant difference to the derived shape of the whole chain. In Fig. 12, we construct the chain using the parameters of Table 5 with either Gaussian (*a*) or uniform monolayer fragments (*b*). The dashed lines in the figure show for comparison the distributions obtained by the simpler analysis of Fig. 6(*c*). It can be seen that the more accurate distribution is very slightly skewed because the chain is more vertically aligned in the region where it starts to overlap the water and head-group distributions. However, a Gaussian remains a very good approximation for the overall chain distribution. This is important for the validity of the assumption that chain and head are described by even functions, which makes the analysis *via* (49) and (50) possible.

5. The resolution of the reflection experiment

The normal criterion for the resolution of a scattering experiment is that it is determined by the maximum momentum transfer, *i.e.* π/κ_{max}, which for neutrons, since κ_{max} is typically about 0.3 $Å^{-1}$, corresponds to a rather poor resolution of about 10 Å. The resolution of the X-ray experiment is up to about three times better. The claim implied by the discussion in the previous section is that the distribution of a fragment can be determined with a considerably higher resolution than π/κ_{max} and we now demonstrate that this is the case.

The argument that is used to define the resolution of a reflection experiment is based on a standard optical argument (Reynolds, DeVelis, Parrent & Thompson, 1989), which we adapt to the situation pertaining for the C_{16}TAB layer. We assume an analytic distribution of a single component through the interface, for which there are three convenient forms, the δ function, a Gaussian (24) and a uniform layer. The corresponding structure

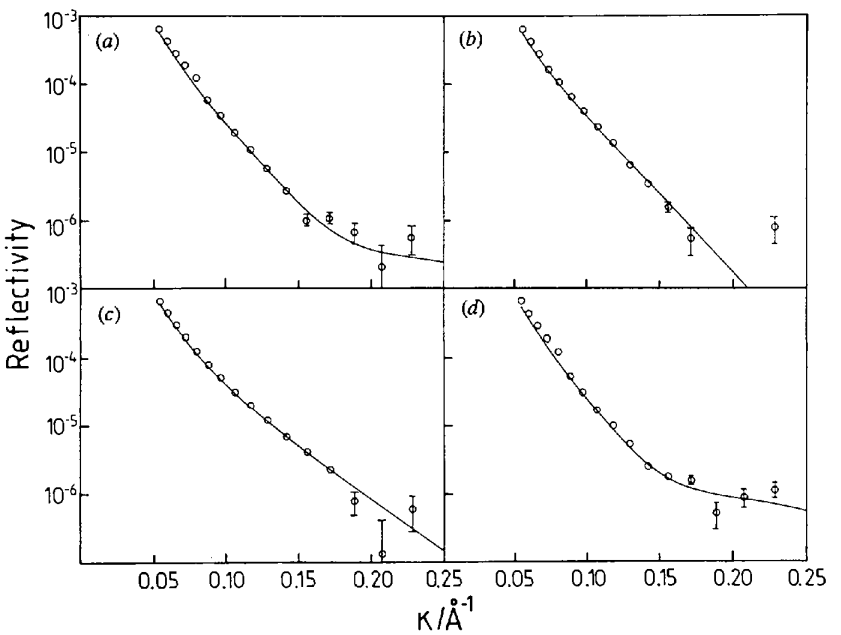

Fig. 11. Part of the simultaneous least-squares fitting of 45 different isotopic compositions of a monolayer of C_{16}TAB adsorbed at the air/water interface. The profiles shown are the neutron reflectivities of '0'$C_{4m}dC_4$'0'$C_{12-4m}h$TAB in D_2O with m = (*a*) 0, (*b*) 2, (*c*) 3, (*d*) 1. The parameters used in the fit are those of Table 5(*b*).

factors are respectively given by

$$h_{ii}^{(1)}(\kappa) = \kappa^2/A^2 \tag{61}$$

and (53) and (54). The smallest measurable thickness is determined simply by whether either of the layer functions can be distinguished from a δ function. A reasonable approximate criterion is that the difference is say 50% of the value for the δ function at κ_{max}, *i.e.*

$$\ln 2 = -\sigma_{min}^2 \kappa_{max}^2/8 \tag{62}$$

or $\sigma_{min} \geq 2.3/\kappa_{max}$, which is comparable with the normal resolution criterion of π/κ_{max}. Fig. 13 compares plots of the structure factors for a δ function and a Gaussian at the same area per molecule such that, at a typical κ_{max} of 0.3 Å^{-1}, the Gaussian is about 50% of the δ function. Under the particular conditions specified, the experimentally determined thickness of any layer thinner than about 8 Å would simply be the resolution limit. We consider some actual data in Fig. 14 where (53) is plotted with three different values of σ and the partial structure factor for the head group of C_{16}TAB. Since only the head group is deuterated, the reflected signal is low but the thickness of the layer is just large enough for it to be reasonable to conclude that the thickness of the layer is 14 (3) Å, though the error would be larger if the area per molecule, which also affects the value of the partial structure factor, were uncertain. The statistics would be better for a more strongly reflecting layer and hence a lower thickness could be determined, but it is clear that the crystallographic resolution of π/κ_{max} applies in a simple reflectivity experiment.

When we examine the possibility of distinguishing two closely spaced distributions in the layer, the situation becomes somewhat more complicated. We use (49), (53) and (61) to derive expressions for the reflectivity when the two distributions are either identical δ functions or identical Gaussians. Thus, for two δ functions

$$h_{tot}^{(1)}(\kappa) = 2\kappa^2/A^2(1 + \cos \kappa\delta) \tag{63}$$

and for two Gaussians

$$h_{tot}^{(1)}(\kappa) = 2\kappa^2/A^2(1 + \cos \kappa\delta) \exp(-\sigma^2\kappa^2/8), \tag{64}$$

where we have again used δ to denote the separation of the two distributions (of individual width σ) and we

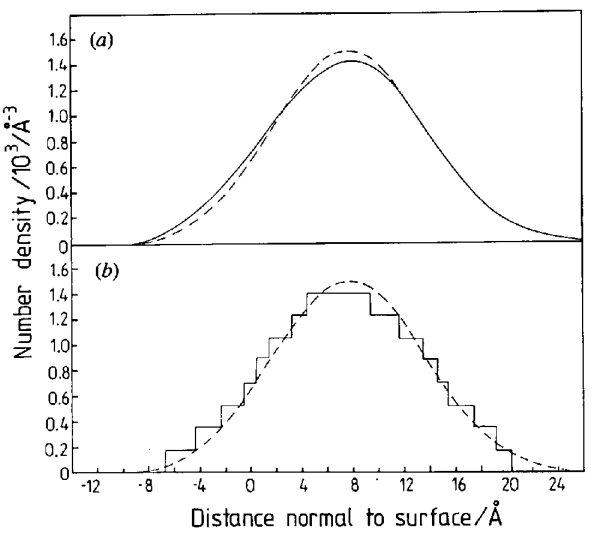

Fig. 12. Distribution of the chain for a monolayer of C_{16}TAB adsorbed at the air/water interface, calculated from the separate C_2 fragments and the experimental values of δ (Table 4), taking each C_2 fragment to be (*a*) a Gaussian distribution of width 14 Å and (*b*) a uniform block of width 16 Å. The dashed line is the experimental Gaussian distribution determined from the experiment when the chain is taken as a single unit.

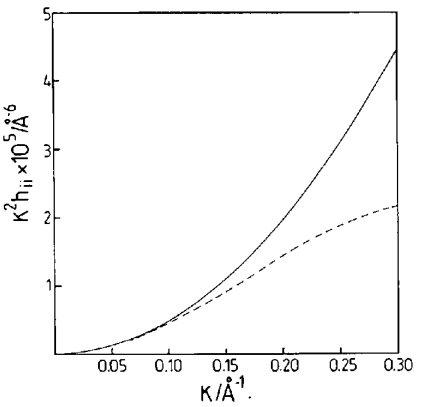

Fig. 13. The partial structure factors for a δ function [continuous line, equation (61)] and Gaussian [dashed line, equation (53)]. The coverage is the same in each case and the thickness is 8 Å for the Gaussian distribution. At the level of signal typical of the deuterated head group of C_{16}TAB at an area per molecule of 45 Å^2, the two functions in the figure would just be experimentally distinguishable.

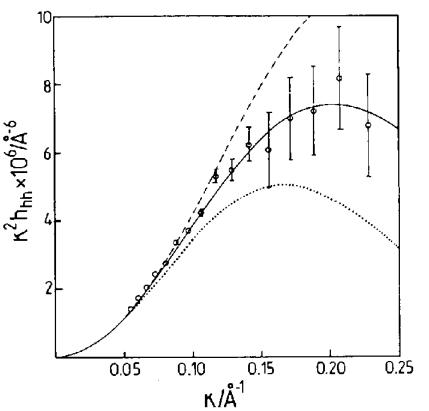

Fig. 14. Comparison of the experimental head-group partial structure factor for a C_{16}TAB monolayer with calculated Gaussians of widths 11 Å (dashed line), 14 Å (continuous line) and 17 Å (dotted line). The area per molecule has been taken to be the same in each case.

have assumed the positive sign in (49) for convenience. Although both these functions now vary more rapidly with κ than for the simple distributions, because the layer is thicker, the important question is whether either function can be distinguished from one of the equations for a single distribution, *i.e.* can it be concluded that there are two distributions, not one. In practice, this comes down to the question as to what κ range is necessary to distinguish the $(1 + \cos\kappa\delta)$ term from a Gaussian because if we cannot distinguish the structure factor (63) from a single Gaussian then we shall certainly not be able to make the distinction when we have the structure factor (64). After allowing for the extra reflectivity from having two groups combined into a single Gaussian distribution, which introduces a factor of four into (53), we then compare (53) and (64) in Fig. 15. Approximately, the two types of profile cannot be distinguished until the $\cos^2(\kappa\delta/2)$ term is close to zero, *i.e.* when $\delta = \pi/\kappa$. Thus, $\delta_{\min}$, the minimum separation of two δ functions that can be distinguished as two separate distributions, is approximately $\pi/\kappa_{\max}$, and once again we recover the usual criterion for resolving two objects optically (Reynolds, DeVelis, Parrent & Thompson, 1989).

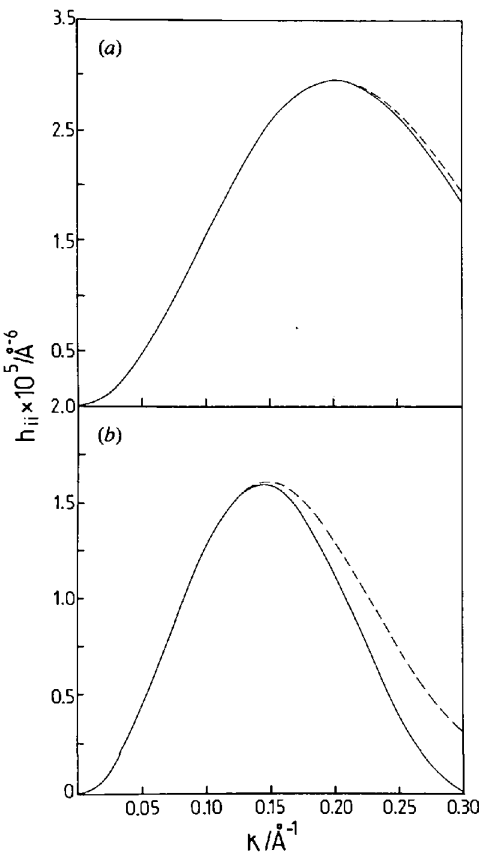

Fig. 15. The difference between two Gaussian distributions separated by a distance δ and one Gaussian. The continuous line is the calculated partial structure factor for two Gaussians [equation (66)] separated by (*a*) 5 and (*b*) 10 Å. The dashed lines are the best fits of a single Gaussian [equation (53)] to the continuous lines, where the fitting has been chosen to be closest at low κ because of the errors in the experimental data being lower in this region. (*b*) represents approximately what would be resolvable in an experiment.

The situation changes dramatically when one is able to make suitable variations in the contrast. Thus, suppose a set of three measurements has been made, which leads to the three component partial structure factors of either (63) or (64). For simplicity, we take the two Gaussians or δ functions to be identical. The $h_{ii}^{(1)}(\kappa)$ are the same as (61) and (53) and after subtraction we obtain the cross term of each partial structure factor:

$$h_{ij}^{(1)}(\kappa) = (\kappa^2/A^2)\cos(\kappa\delta)$$
$$= \pm h_{ii}^{(1)}(\kappa)\cos(\kappa\delta) \quad (65)$$
$$h_{ij}^{(1)}(\kappa) = (\kappa^2/A^2)\cos(\kappa\delta)\exp(-\sigma^2\kappa^2/8)$$
$$= \pm h_{ii}^{(1)}(\kappa)\cos(\kappa\delta). \quad (66)$$

The interference term is now entirely independent of the shape of the distributions and therefore the criterion for resolving the two distributions becomes a question of the accuracy with which the fitting of the $\cos(\kappa\delta)$ term to the data gives δ. There is now no problem of having to make a choice between different functional forms of the structure factor. Thus, in principle, there is no limit to the value of δ and even two δ functions only 1 Å apart could be distinguished, although as δ decreases so the relative accuracy decreases because $\cos(\kappa\delta)$ varies more slowly with δ for small δ. This holds, even though the distributions cannot themselves be determined with such high resolution. In practice, the quality of the data may limit the accuracy and hence the resolution, but this is more likely to result from systematic errors, which we consider further below. The important conclusion is that, by measuring the distances between distributions, the resolution of the experiment can be enhanced by nearly an order of magnitude. The conclusions about the resolution are not affected by a change to even and odd distributions (50) other than through differences in the statistical quality of the data. In simple optical terms, the reason that the resolution can be so enhanced by the partial-structure-factor measurements is given in Fig. 16. Two Gaussian distributions separated by a distance less than their widths are shown in Fig. 16(*a*) and the sum of the two (Fig. 16*b*) can also be fitted with a single Gaussian within error. It is therefore impossible to distinguish whether there are two distributions or one wider one. If the width of each distribution is determined separately, then this result may be combined with the whole distribution to obtain the separation (Fig. 16*c*). The partial-structure-factor method not only does this but goes somewhat further and extracts the interference function between the two distributions directly.

In terms of the resolution criteria described above, it must now be clear that, because of the wide difference

in the effective resolution being used to determine the σ_j on the one hand and the δ_{ij} on the other, the errors in the σ_j values should be much larger. This is borne out by the data in Tables 1–5 where the δ_{ij} values remain within a narrow error band whatever the constraints imposed, whereas the σ_j values, especially when the fragment size is small, are very sensitive to any applied constraints. Since, in general, the δ_{ij} values contain the most interesting information about the interfacial structure, the best design for an experiment is to focus on the δ_{ij} rather than the σ_j. This observation also accounts for an interesting feature that one notices when analysing a set of isotopic data, which is that the introduction of roughness as a fitting parameter often has little effect on the final structure determined in a neutron experiment, whereas it is often very important in X-ray reflectivity. The introduction of roughness has no effect on the δ_{ij}, but does affect the σ_j. The σ_j and the roughness are strongly linked and the low resolution of the neutron experiment means that they may not be clearly distinguished, unless of course the dimensions of the layer are larger than about 50 Å. The X-ray experiment is generally more sensitive to the overall thickness and with its considerably higher resolution will often be able to determine the roughness as an independent parameter.

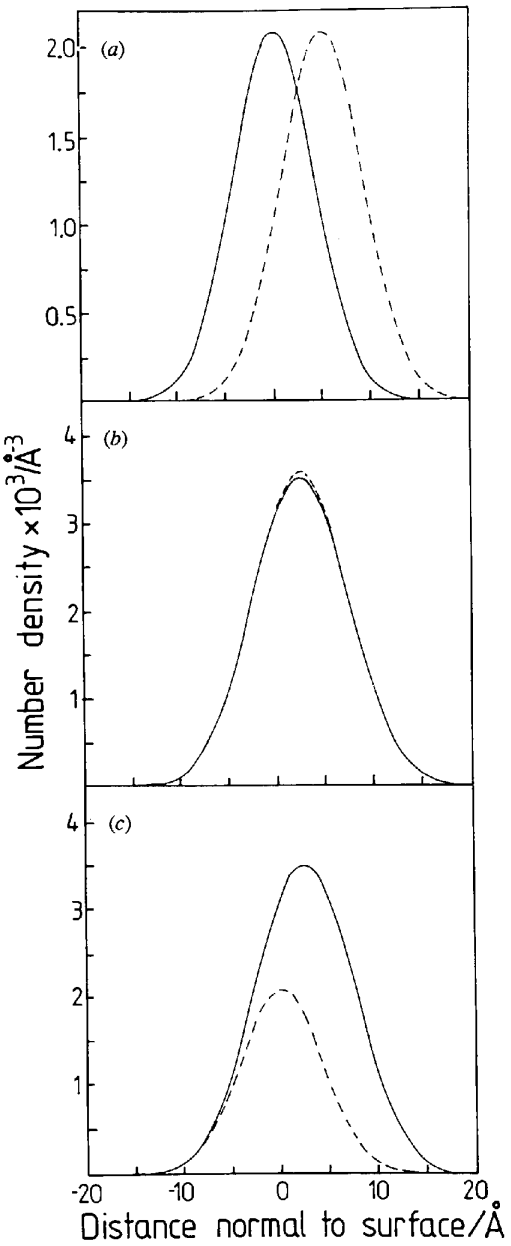

Fig. 16. (*a*) Two identical Gaussian distributions of width 12 Å separated by 5 Å and whose sum is the continuous line shown in (*b*) and (*c*). The dashed line in (*b*) is the best fit of a single Gaussian to the sum of the two Gaussians from (*a*) and shows that, under these circumstances ($\delta < \sigma/2$), the existence of the two component Gaussians cannot be distinguished. If one of them can be measured separately, as shown schematically in (*c*), the existence of the two can be deduced by subtraction of one Gaussian from the total.

6. Roughness

Most real interfaces are rough, liquids because of thermal motion and solids because of static roughness. In addition to the roughness, there may be a finite distance over which the density changes between the two limits of the bulk phases, which we refer to as the diffuseness of the interface. Roughness and diffuseness both reduce the specular reflectivity, the latter being just a reduction but the former removing signal from the specular to the off-specular direction. For a simple liquid, the effects of roughness and diffuseness on the specular reflectivity cannot be distinguished but can only be resolved by off-specular measurements (Braslau, Deutsch, Pershan, Weiss, Als-Nielsen & Bohr, 1985) and, since the roughness transfers signal from specular to off-specular scattering, the effect of roughness on the specular intensity depends on the instrumental resolution. These effects have been considered in some detail by Braslau *et al.* (1985) and Schwartz, Schlossman, Kawamoto, Kellogg, Pershan & Ocko (1990). Since we are here only considering specular reflection, we make no attempt to distinguish diffuseness and roughness but lump them together under the single term 'roughness'.

Roughness is often used as a fitting parameter in modelling specular reflectivity profiles and is easily included in the optical matrix calculation (Cowley & Ryan, 1987). For a fitted roughness parameter to have any physical significance, the resolution has to be sufficiently high to distinguish its effect on the reflectivity. Given the discussion in the earlier sections, this means that, in terms of a single layer, κ_{max} must be large enough to observe the damping of the partial structure factor (see Fig. 7). Thus, even the observation of one complete interference fringe from a uniform layer may not be

sufficient to define the roughness uniquely. It is worth noting that, although neutron reflection may not have sufficient resolution to determine the roughness from the damping of any interference fringe, except when the layer thickness is greater than about 50 Å, the method of progressively increasing the length of the label does give a direct measurement of the roughness (Fig. 9). The question we address here is whether the roughness propagates uniformly through the layer. Thus, there must be some depth in the solution where the system is no longer following the thermal motion of surfactant at the air/liquid interface.

In evaluating the form of the cross partial structure factor [(49) and (50)], we have assumed an *average* distribution of the two separate components contributing to the cross term, *i.e.* the interference is between the two average distributions and there are no losses resulting from coupling of the distributions to in-plane fluctuations. This is not necessarily correct and it may be necessary to introduce an additional damping term to allow for these fluctuations. Pershan (1994*a*) has observed such a damping effect for relatively thick (of the order of hundreds of Å) helium layers on a solid substrate. Pershan's modification of the specular reflection in the presence of such damping would modify the expressions for the cross terms given earlier to

$$h_{ij}^{(1)}(\kappa) = \pm[h_i^{(1)}(\kappa)h_j^{(1)}(\kappa)]^{1/2}\cos(\kappa\delta_{ij})\exp(-\tfrac{1}{2}\kappa^2\varepsilon_{ij}) \tag{67}$$

and

$$h_{ij}^{(1)}(\kappa) = \pm[h_i^{(1)}(\kappa)h_j^{(1)}(\kappa)]^{1/2}\sin(\kappa\delta_{ij})\exp(-\tfrac{1}{2}\kappa^2\varepsilon_{ij}), \tag{68}$$

where ε_{ij} is a damping factor. In the surfactant layers under consideration, such a damping term could arise between the water substrate and the surfactant layer if the thermal motion of the surface in the vertical direction were not uniform through the surface. If at some depth in the underlying liquid the thermal motion is no longer correlated with that of the outer part of the layer, there will be damping effects that will lead to errors in the values of the δ_{ij} deduced from the experiment.

We first note that the presence of a damping term would not only affect the analysis in terms of partial structure factors but would make the optical matrix calculation of the reflectivity incorrect. This would lead to errors in *all* the methods of analysis discussed in this paper! It is therefore important to have some means of establishing whether or not the effect is significant. In terms of the partial-structure-factor analysis of the surfactant layer, it is relatively easy to detect. Fig. 17 shows the effects of introducing finite values of ε_{ij} into cross partial structure factors of the two types, (*a*) between two parts of the surfactant molecule and (*b*) between a surfactant fragment and water. By comparison with (28), an appropriate value for ε_{ij} might be of the order of σ^2 for water, *i.e.* about 9 Å^2, and the calculations shown in Fig. 17 are based on this value. As would be expected, the effect of the damping is to reduce the cross interference. This changes the shape of the cross partial structure factor and, if the effect is large, it will not be possible to fit the simpler equation (49) to the data. The value of ε_{ij} of 9 Å^2 already has this effect in Fig. 17. However, when experimental error is included, or when the observed cross term has not reached a maximum or minimum, *i.e.* $\kappa\delta_{ij}$ is small, the contribution of damping would not be distinguished from a slightly smaller value of δ_{ij}. Thus, when experimental error is included into Fig. 17 the fitted values of δ_{ij} when damping is occurring would be about 1 Å (about 10%) smaller than their values in the absence of damping. This then implies that, if damping is present, the values of δ_{ij} obtained from fitting the data, whether by partial-structure-factor analysis or by use of the optical matrix model, will be *underestimates* of the true values. It seems probable that damping effects might become more significant as the separation of the fragments increases

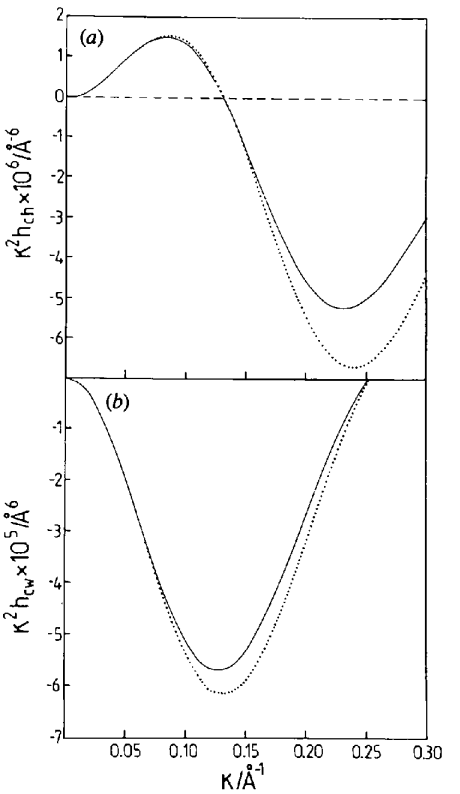

Fig. 17. Damping effects [equations (67) and (68)] on the determination of the separations of distributions using two types of cross partial structure factors (*a*) between two even distributions and (*b*) between an odd and an even distribution. The dotted lines are calculated partial structure factors with structural parameters typical of the C_{16}TAB monolayer (δ_{ch} = 12 and δ_{cw} = 12.5 Å. The continuous lines include a damping factor ε of 9 Å^2 and have an effect equivalent to changing the δ values by about 1 Å or 10% of δ.

or when considering components that are not directly attached to one another, *e.g.* water and surfactant. Thus, the overdetermination of the separations between the different components of the interface should help to identify the damping effect because they will lead to inconsistencies. For the C_{16}TAB system being considered here, we have observed no detectable damping effects, indicating that the water interface moves with the surfactant.

The effect of damping on the reflectivity itself can be deduced using the partial-structure-factor analysis. In the case of Fig. 17(*a*), the magnitude of the positive cross term is decreased by damping as κ increases. Through (67), this leads to a reduction in the reflected signal, which increases with κ. This gives an apparently thinner layer, as found above and, if the reflectivity cannot be extrapolated to $\kappa = 0$, an apparently lower amount of material at the surface. Thus any experimental result indicating that the amount of adsorbed material is less than expected may also be indicating that damping effects are significant. It is then essential to make accurate measurements down to as low a κ as possible. Since terms of the type shown in Fig. 17(*b*) are negative, damping in this case causes the reflectivity to be increasingly larger than expected as κ increases. The effect of this on the analysis is then difficult to predict because it depends on the scattering-length densities of both the layer and the substrate.

7. Partial structure factors and the phase problem

It is always possible to describe the structure of the interface in terms of odd and even distribution functions. Given limited *a priori* knowledge of the system, the only phase ambiguities then occur in the cross terms in the partial structure factors, *i.e.* the sign ambiguities in (49) and (50). Thus, the phase problem manifests itself as an ambiguity in the sign of each value of δ_{ij}. However, there will always exist relations of the type of (52) which link the various δ_{ij}. It should then be possible by overdetermination of the structure in terms of the number of partial structure factors to resolve the phase problem to a level that physical reasonableness or knowledge of the structure completes an unambiguous determination. The simplest example of this is the structural relation of heads, chains and water for the coarse labelling of the C_{16}TAB layer. Each determined δ_{ij} may be positive or negative and the only possible solutions are with the hydrocarbon chain pointing away from the water and being slightly further from the water than from the head group (see Table 1 for the values of δ_{ij}), or that the hydrocarbon chain is totally immersed in the water with the head group at the surface and slightly immersed in the water. The latter is obviously physically unreasonable and so the structure is unambiguously determined. Phase ambiguity may, however, remain because of limitations on the resolution. As described in the section on resolution, relative errors in the δ_{ij} increase as δ_{ij} becomes small because the resolution limit is being approached. Thus, the uncertainty in δ_{hw} in the coarse determination of the C_{16}TAB structure is such that it is only just accurate enough to decide which way round are the head-group and water distributions. This ambiguity was also the reason for introducing the constraint of no backfolding in the C_{16} chain when doing the least-squares fit to the set of 45 profiles involving C_2 fragments. The quite large error in each δ_{nh} made it possible for the program to lock in to minima where the δ_{nh} might be in the wrong order, *i.e.* to choose the wrong phases.

8. Systematic errors

There are two main sources of error in the determination of reflectivity, the background subtraction and systematic errors resulting from non-reproducibility, isotope effects *etc.* Isotope effects do not matter unless a set of reflectivities is being used and the contribution of the background is much more of a problem for neutrons than for X-rays. The experimental problem of the background subtraction is that the background cannot strictly be determined. It is obtained either by extrapolation to each side of the specular peak or by extrapolating to essentially zero reflectivity, *i.e.* to the total signal at high κ. The latter is only a valid procedure when the background is known to be flat. In the special case where the components forming the bulk phases can be contrast matched and where the interface can also be made null reflecting the background resulting from incoherent and multiple diffraction effects, which are the main contributors to the neutron background, can be determined experimentally. However, the true background may still have off-specular components which do not totally vanish under these contrast conditions. We have previously discussed the effects of errors on the partial-structure-factor method (Lu, Simister, Thomas & Penfold, 1993*a*) but with the possibility of the simultaneous fitting of a whole set of isotopic profiles and a clearer understanding of the factors determining the resolution of the experiment, it is useful to re-examine the problem. For simplicity, we do this for the case of a flat background only.

The effect of the subtraction of an incorrect background level is most easily assessed starting from Fig. 14, which shows the determination of a self partial structure factor whose width is close to the resolution limit, as defined by π/κ_{max}. We assume that there is a constant background error of Δ, which will give rise to an error in $h_{nn}^{(1)}$ of

$$E = \kappa^4 \Delta / 16\pi^2 b^2. \tag{69}$$

The largest background in solution work is usually obtained when null reflecting water or H_2O is the sub-

strate and is typically about 6×10^{-6} (measured in terms of the reflectivity). If 5% of this is taken as a reasonable error, then, for the scattering length of a small fragment of the type shown in Fig. 14 at $\kappa = 0.15\,\text{Å}^{-1}$, E is about 2×10^{-6}. This is a significant error and, as can be seen from Fig. 18 where we plot the experimental partial structure factor with different subtracted flat backgrounds, would lead to a large error in the determined width of the distribution. The results of the fitting in Fig. 18 reinforce the earlier conclusion that, when the scattering-length density of a fragment is small, *e.g.* it contains less than the equivalent of about ten close-packed D atoms, its width cannot be determined to better than about 30%. This is the reason for the inaccurate values obtained for the widths of the head group, C_4 and C_2 fragments in Table 5 and of the head group in Table 1. The reflectivity profiles are just not very sensitive to the thickness of the distribution at this low signal level. This makes it doubly important that an independent measure of the thickness of these fragments can be made as in Fig. 9. Although each of the measurements in Fig. 9 is susceptible to the same type of background error, the relative error rapidly becomes smaller as the number of labelled atoms increases, the signal increasing as the square of the number of C and D atoms in the labelled fragment. Provided that a reasonably linear extrapolation may be made, the determination of the limiting fragment thickness by this means will be much more accurate than by determination from an individual partial structure factor.

It is less easy to determine the effect of errors on the cross partial structure factors because of the way that these errors may propagate through the various data manipulations that take place. At first sight, background-subtraction errors play at least an important part as for the self partial structure factors. Thus, a typical cross term (in null reflecting water) is obtained by

$$2b_n b_h h_{nh}^{(1)} = (\kappa^4/16\pi^2)[R_{nh} - R_h - R_n], \qquad (70)$$

where R_{nh} and R_h are the reflectivities when groups n and h and group h are labelled, respectively. The background errors would then appear to be comparable with the errors in the self partial structure factors. However, in the fitting of δ_{nh} values there is not as much emphasis on the high-κ region where the background errors are largest and it is generally found that the values obtained for the δ_{nh} are not as sensitive to this type of error. In fact, the δ_{nh} are more sensitive to other systematic errors such as non-reproducibility, calibration of the intensity and small isotope effects. To illustrate this, we choose the simple case where $b_n = b_h$, $R_{nh} = 4R_h$ and $R_h = R_n$. We suppose that there is a 5% error in the coverage, which is equivalent to a 10% error in R_h. It is then easy to show using (70) and (49) that

$$h_{nh}^{(1)} = h_{hh}^{(1)}[\cos \kappa\delta_{nh} \pm 0.05]. \qquad (71)$$

In the middle of the useful range of κ and for a typical value of δ_{nh} of 5 Å, this gives rise to an error of about 0.5 Å. The relative error will increase as δ_{nh} increases and it will also increase if more weight is given to the points at highest κ. However, this error in the determination of a single δ_{nh} can be reduced in two ways. The first, and most obvious, way is for the set of independent δ_{nh} to be overdetermined as has been done in the present work on C_{16}TAB. Since the errors of the type described by (71) are random and since as much attention is given to determining the smaller δ_{nh} values as to the larger ones, the overdetermination will greatly reduce the errors in the individual δ_{nh} and this is reflected in the errors produced in the tables by the non-linear least-squares-fitting routine. A second procedure for reducing these systematic errors starts by acknowledging that all the sources of error other than the background subtraction have the effect that the apparent coverage fluctuates about the correct value. Some improvement can then be obtained by determining the average coverage from the whole set of data (the coverage is model independent to a high degree of approximation) and rescaling the reflectivity of each profile to give the correct average coverage. This reduces to a minimum the 'cross talk' between the self and cross terms in the partial structure factors that leads to the errors of (71). This procedure has been followed in the determination of the δ_{nh} values from the partial structure factors. The test of the success of such a procedure is that in cases where the structure is overdetermined it gives a more self-consistent set of data. The equivalent correction in the least-squares fitting of the set of reflectivity profiles is to constrain the area per molecule to the average value obtained from the set

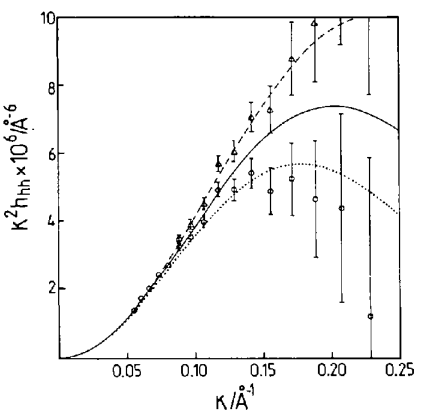

Fig. 18. Effect of background errors on the calculated thickness for the head-group partial structure factor for a monolayer of C_{16}TAB adsorbed at the air/water interface. The lines are calculated for Gaussian distributions of width 11 Å (dashed line), 14 Å (continuous line) and 17 Å (dotted line). The data points obtained with the best fitted background would best be fitted by the continuous line (see Fig. 14). The two sets of points shown are with ±5% changes in the subtracted background.

of data in null reflecting water, and we have already noted the value of this constraint.

The discussion of the resolution and systematic errors in the reflection experiment as applied to the C_{16}TAB monolayer show that it is possible to determine with acceptable accuracy the separation of components in the layer provided that they give an adequate signal. At the surface coverages used, the C_2 fragments appear to be just too small as is evident from the values of δ_{nh} in Tables 4 and 5 in comparison with the errors but the experiment is possible in terms of C_4 fragments.

A final source of systematic error is the assumption of specific analytic forms for the distributions of each component of the layer and the related assumptions of evenness and oddness in applying (49) and (50). Since any distribution may be expressed in terms of a series of simple distributions, it is always possible to use a more complete set of basis distributions to explain a set of reflectivity profiles. This also extends to using mixtures of odd and even functions to describe a distribution. A mixture of odd and even distributions would be needed, for example, to describe the distribution of ethanol adsorbed at the surface of ethanol/water mixtures (Li, Lu, Styrkas, Thomas, Rennie & Penfold, 1993). However, the inclusion of extra terms introduces more fitting parameters and would destroy the main attraction of the use of partial structure factors, *i.e.* that they give a simple interpretation of the structure in terms of intuitively reasonable descriptions of the distributions of the individual components. Some analysis of the errors arising from the use of (49) and (50) when the distributions are not exactly even or odd has been given (Simister, Lee, Thomas & Penfold, 1992*a*,*b*), which shows that the approximation holds best at low $\kappa\delta$, although the very slight deviation from evenness of the distribution in Fig. 12 would not contribute any error over the range of κ explored in the experimental results described here.

9. Partial structure factors in the absence of labelling

We have so far used the partial-structure-factor method as a means of comparing different reflectivities from the same chemical structure. However, as implied by Denton, Gray & Sullivan (1994), partial structure factors may be the simplest approach to the interpretation of the reflectivity even when there is no isotopic data. Lu *et al.* used such an approach to interpret longer-range structure at the air/water interface of a surfactant solution above its critical micelle concentration (c.m.c.) (Lu, Simister, Thomas & Penfold, 1993*b*). The surfactant was found to form the usual monolayer at the surface and a layer of micelles (or aggregates of some kind) also formed at some distance below the surface. For the deuterated surfactant in null reflecting water, the reflectivity therefore contains three terms:

$$R_1 = (16\pi^2 b_a^2/\kappa^4)\left[h_{mm}^{(1)} + h_{11}^{(1)} + 2h_{m1}^{(1)}\right], \qquad (72)$$

where the subscripts m and 1 denote monolayer and micellar layer, respectively. The number of excess micelles was estimated to be small and such as to make the $h_{11}^{(1)}$ term in (72) negligible in comparison with the the other two terms. A measurement of the reflectivity at the c.m.c., $R_{\rm cmc}$, where there are no micelles, gives an approximate measure of $h_{mm}^{(1)}$. Hence,

$$h_{m1}^{(1)} \simeq (\kappa^4/32\pi^2 b_a^2)[R_1 - R_{\rm cmc}] \qquad (73)$$

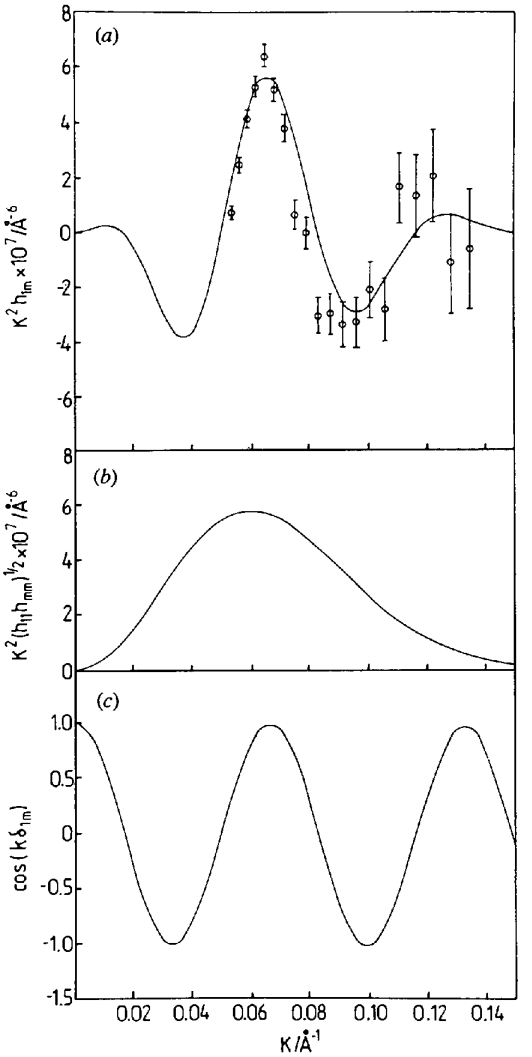

Fig. 19. Approximate cross term in the partial structure factor between a surfactant monolayer and a layer of micelles below the surface [equation (74)]. The two contributing factors to the partial structure factor are shown in (*b*) and (*c*). The overall fit to the data is shown in (*a*). The thickness of the micellar layer is 65 Å centred about 95 Å from the monolayer at the surface.

and taking Gaussian distributions for both monolayer and micellar layer,

$$h_{m1}^{(1)} = (\pi\sigma_m\sigma_1 n_m n_1/4)\kappa^2 \exp\left[-\kappa^2(\sigma_1^2 + \sigma_m^2)/8\right] \times \cos\kappa\delta_{1m}, \quad (74)$$

where δ_{1m} is the separation of micellar and monolayer. Fig. 19 shows the contribution of the two main terms in (74), the composite Gaussian and the cos term, to the observed partial structure factor. Although this is only an approximate interpretation, a more refined calculation hardly changed the fitted parameters. The value of using analytical forms for the two self partial structure factors here is that it gives a direct physical interpretation of the main features of the reflectivity with minimal use of fitting routines.

10. Isotope effects

As should be clear from some of the preceding discussion, the partial-structure-factor method does not have to rely on data from different isotopic species. Thus, an improvement in the quality of the information obtained from specular reflectivity will result from choosing the isotopic composition to optimize the neutron reflectivity and then combining the neutron reflectivity data with X-ray measurements on the same sample. The more common situation will utilize data from samples of different isotopic composition. The danger is then that there may either be genuine isotope effects where one pure isotopic species behaves differently from another or there may be secondary isotope effects because it is not possible to reproduce a given system accurately or because there are differences in the purity or chemical formulae of the isotopic species.

For the soluble surfactant systems used as illustration throughout this review, surface-tension measurements indicate that genuine isotope effects are negligible and it is relatively straightforward to prepare the interfacial system reproducibly to within about 5% in terms of amount of material at the interface. Thus, provided that the labelled systems studied give reflectivities that differ by substantially more than about 5%, the method should be accurate. If the differences are comparable with the reproducibility, the direct determination of the partial structure factors is likely to blow up and give ridiculous values of the structural parameters. The use of the partial structure factors to fit the reflectivity directly relaxes the reproducibility requirement in that the partial structure factors are not determined explicitly and the method is not as vulnerable to a pair of ill conditioned reflectivity profiles. There are many systems where there may be no routine method for establishing the lack of an isotope effect, in which case, the measurement of the X-ray reflectivity may be a useful means of testing isotope dependence of the interfacial structure [see, for example, (Styrkas, Thomas, Adib, Davis, Hodge & Liu, 1994)].

There are a number of interfacial systems for which isotope effects have been reported. These are likely to occur when a system is near a phase transition. What might then be a small isotope effect on, say, the absolute temperature of the phase transition may cause substantial differences in the interfacial properties of the two isotopic species near that phase transition. Such effects are more probable, and have been reported, for closely packed monolayers. It is also well known that polymeric systems may have significant isotope effects (Atkin, Kleintjens, Koningsveld & Fetter, 1984) but the more serious problem with polymeric systems is often that it is exceedingly difficult to prepare identical polymer molecules. The solution to this problem may then be to prepare a series of samples and to try to find pairs of isotopic species with the same properties. Finally, it is worth mentioning our own experiences in attempting to use the partial-structure-factor method for solid/liquid interfaces.

The solid/liquid interface is generally more complex than the air/liquid interface. For example, a typical experiment might attempt to determine the structure of a surfactant layer adsorbed on hydrophobically coated silicon. If any isotopic substitution is to be used on the hydrophobic layer, and there are good reasons for wanting to do this [see, for example, Fragneto, Thomas, Rennie & Penfold (1995)], the reproducibility of the surface roughness and the condition of the natural oxide layer, both of which may affect the hydrophobic layer on the silicon, may not be high enough to extract partial structure factors with certainty. Thus, we have so far not succeeded in applying the partial-structure-factor method to any data at the solid/liquid interface, even though we have made the theoretical number of isotopic substitutions necessary. It is probable, however, that the direct fitting routine will prove more effective for this problem.

11. Conclusions

We have aimed to show that the labelling of suitably chosen fragments of an interface may be used to probe its structure much more effectively than would be possible from a reflectivity measurement on unlabelled species. We now attempt to set the method in the context of the various methods that have been used to analyse reflectivity data up to now. We represent these schematically in Table 6 and in terms of an idealized common treatment for each approach, excluding those methods that aim for a truly direct inversion of reflectivity data, *i.e.* the experiments of Sanyal *et al.* (1993) and Penfold, Webster, Bucknall & Sivia (1994), and the proposed method of Feideldy, Lipperheide, Leeb & Sofianos (1992), none of which is expected to be of general utility.

Table 6. *Summary of main methods for relating reflectivity to interfacial structure*

Basis	Method for phase problem	$P^{(1)}(z)$	$\rho(z)$	$n(z)$	Reference
(Direct Fourier transform)	–	$P^{(1)}(z)$	–	–	*(a)*
Cubic b splines	**Square root deconvolution**	–	$\rho(z)$	–	*(b)–(e)*
Periodic functions	**(Not separate)**	–	$\rho(z)$	–	*(f)*
Uniform layers (min.)	**(Not separate)**	–	$\rho(z)$	–	*(g)*
Uniform layers (max.)	**(Not separate)**	–	$\rho(z)$	–	*(h)*
Uniform layers (max.)	**Non-linearity**	–	$\rho(z)$	–	*(i)–(k)*
Basic chemical fragments	*(Not separate)*	–	–	$n(z)$	*(l)*
Partial structure factors	*Structural relations*	–	–	$n(z)$	*(m)–(s)*

The bold type indicates that an exact relation between reflectivity and scattering-length-density profile is used, italics that the relation is approximate (kinematic or corrected kinematic). References: *(a)* Pershan (1989); *(b)* Pedersen (1992); *(c)* Hamley & Pedersen (1994); *(d)* Pedersen & Hamley (1994*a*); *(e)* Pedersen & Hamley (1994*b*); *(f)* Singh, Tirrell & Bates (1993); *(g)* Sivia, Hamilton & Smith (1991); *(h)* Kunz, Reiter, Götzelmann & Stamm (1993); *(i)* Zhou & Chen (1993); *(j)* Zhou, Lee, Chen & Strey (1992); *(k)* Zhou & Chen (1995); *(l)* Denton, Gray & Sullivan (1994); *(m)* Crowley, Lee, Simister & Thomas (1991); *(n)* Lee & Milnes (1995); *(o)* Lu, Hromadova, Simister, Thomas & Penfold (1994); *(p)* Lu, Simister, Lee, Thomas, Rennie & Penfold (1992); *(q)* Lu, Simister, Thomas & Penfold (1993*a*); *(r)*, *(s)* Simister, Lee, Thomas & Penfold (1992*a*,*b*).

For the purposes of comparison, it is convenient to think of all these fitting procedures as being divided into three steps, although this may not be how they are actually executed. The first step is either a direct Fourier transform or the fitting of a set of basis functions to the reflectivity (the indirect Fourier transform or an equivalent) to give a Patterson function. The second step is the solution of the phase problem, either a deconvolution of the Patterson or some means of putting phase information into step one so that a reliable scattering-length-density profile is obtained. The third step, to which much less attention has been given, is the determination of the actual composition profile from the scattering-length-density profile determined in the first two steps.

The most widely used method is to calculate the reflectivity using a model of a series of uniform layers and to compare it with the observations. The three steps given above are then inextricably entangled and this often makes it difficult to assess what is required to improve a fit or to establish the uniqueness of a given interfacial structure. A different insight would be obtained if the uniform block distributions were converted to partial structure factors and these fitted to the reflectivity, though this is not usually the procedure used. For n layers there are then $2n$ unknown parameters, the scattering-length density and thickness of each layer (there may be more unknown parameters if the composition profile is to be derived). The separations between the layers, which determine the phases, are defined in terms of the thicknesses if the layers are contiguous. Within the kinematic approximation, the reflectivity can then be expressed analytically using equations (41), (49) and (50) and the observed reflectivity could be fitted directly in the manner of Lee & Milnes (1995). This would be equivalent to fitting a set of n basis functions of predetermined functional form, though of variable width and amplitude, while fitting the phase of the reflectivity by adjustment of the relative positions of the layers. Since the latter are usually directly determined by the thicknesses, any change in one of the functions will also affect the phase. The fitting procedure is therefore more complex than when the analysis is divided into sequential steps, as in the method of Pedersen (1992) and it is not surprising that many researchers find it difficult to fit their data. The further complication is that a set of layers of uniform scattering-length density does not usually map on to a set of chemically distinct layers because one component may be distributed unevenly throughout several layers. It may then be necessary to make further assumptions, including volume and composition constraints, and the relation between the chemical composition and scattering-length-density distributions may not only be complicated but not unique, which further widens the choice of starting models or the choice of models that will fit the data adequately.

The occasions where the uniform layer model is most appropriate will be those when the width of the interface is such that data close to the critical angle are important, *i.e.* the kinematic approximation is invalid, or when the chemical composition is such that it almost divides into uniform layers, *e.g.* a polymer film on a solid substrate. This is when the Bayesian approach of Sivia, Hamilton & Smith (1991) will be most effective. This introduces an objective means for optimizing the selection of the block model basis functions using a minimum number of uniform layers and making use of independent information about the layer when possible. When the composition is such that several uniform layers are required to fit the data, it is not clear, however, that any procedure, however objective, can be generally totally reliable because the implication of needing several layers to describe the system is that it is chemically somewhat complex and then one runs into the problem described in the previous paragraph.

One of the advantages of separating, at least in part, the initial Fourier transform step from the deconvolution of the Patterson is that the basis functions can be chosen

to be more characteristic of the way that the interface is made up and therefore less artificial. Thus, in the method of Singh, Tirrell & Bates (1993), periodic functions are used as the basis set and this is clearly appropriate for multilayer structures.

The distinctive feature of the approaches of Denton, Gray & Sullivan (1994) and Lee & Milnes (1995) is the focus on the chemical elements at the interface and their basis sets are functions chosen to match the chemical description of the interface as closely as possible. The methods of Lee & Milnes and Denton *et al.* are close in spirit to an indirect Fourier transform. In addition, the method of Lee & Milnes also solves the phase problem more or less completely because it makes use of definite phase relations between some of the partial structure factors, and therefore does the equivalent of the square-root deconvolution of Pedersen (1992). Denton *et al.*'s method is tuned to the ultimate chemical logic of the structure of the interface but, since information at this resolution is not usually available, this means that constraints must be included. The method of Lee & Milnes is tuned to the isotopic labelling scheme used for the experiment. The method of Simister, Lee, Thomas & Penfold (1992*a*,*b*) is not substantially different from an indirect Fourier transform with square-root deconvolution but focuses more closely on the set of structural parameters that can be obtained without recourse to detailed models. All three methods in this paragraph are limited to approximations for the reflectivity but have the advantage that they yield the structure, rather than the scattering-length profile, directly. They also rely on the possibility of using more than one reflectivity profile.

It would seem self-evident that if the quality of the data is good and the range of κ is appropriate, the ideal would be to Fourier transform the data directly to obtain the Patterson function. It should now be clear that this does not solve the whole problem, which is to obtain the individual number densities, and this is one of the reasons that this route has not been followed very often [see, for example, Pershan (1989) and Schlossman *et al.* (1991)].

Finally, we draw attention to the fact that we have only discussed *specular* reflectivity. There are likely to be occasions when it becomes difficult to separate specular and non-specular reflection and then it will be essential to use a full model that does not separate the scattering-length-density profile normal to the surface from fluctuations in the surface plane. Although some attempts have been made to move along this route (see Sinha, Sirota, Garoff & Stanley, 1988), theoretical and experimental progress will be necessary before it becomes more widespread.

We thank the Engineering and Physical Science Research Council for support and one of us (EML) thanks the University of Oxford for a Glasstone Fellowship.

References

Als-Nielsen, J. (1985). *Z. Phys.* B**61**, 411–414.

Atkin, E. L., Kleintjens, L. A., Koningsveld, R. & Fetters, L. J. (1984). *Macromol. Chem.* **185**, 377–387.

Böcker, J., Schlenkrich, M., Bopp, P. & Brickmann, J. (1992). *J. Phys. Chem.* **96**, 9915–9922.

Born, M. & Wolf, E. (1970). *Principles of Optics*. Oxford: Pergamon.

Bracewell, R. N. (1978). *The Fourier Transform and its Applications*, 2nd ed. New York: McGraw-Hill.

Braslau, A., Deutsch, M., Pershan, P. S., Weiss, A. H., Als-Nielsen, J. & Bohr, J. (1985). *Phys. Rev. Lett.* **54**, 114–117.

Cowley, R. A. & Ryan, T. W. (1987). *J. Phys. D*, **20**, 61–68.

Crowley, T. L. (1984). DPhil thesis, Oxford University, England.

Crowley, T. L. (1993). *Physica (Utrecht)*, A**195**, 354–374.

Crowley, T. L., Lee, E. M., Simister, E. A. & Thomas, R. K. (1991). *Physica (Utrecht)*, B**173**, 143–156.

Crowley, T. L., Lee, E. M., Simister, E. A., Thomas, R. K., Penfold, J. & Rennie, A. R. (1990). *Colloid Surf.* **52**, 85–106.

Denton, A. R., Gray, C. G. & Sullivan, D. (1994). *Chem. Phys. Lett.* **219**, 310–318.

Dietrich, S. & Schack, R. (1987). *Phys. Rev. Lett.* **58**, 140–143.

Fiedeldy, H., Lipperheide, R., Leeb, H. & Sofianos, S. A. (1992). *Phys. Lett.* A**170**, 347–351.

Fragneto, G., Thomas, R. K., Rennie, A. R. & Penfold, J. (1995). *Science*, **267**, 657–660.

Glatter, O. (1977). *J. Appl. Cryst.* **10**, 415–421.

Guiselin, O., Lee, L. T., Farnoux, B. & Lapp, A. (1991). *J. Chem. Phys.* **95**, 4632–4640.

Hamley, I. W. & Pedersen, J. S. (1994). *J. Appl. Cryst.* **27**, 29–35.

Heavens, O. S. (1965). *Optical Properties of Thin Solid Films*. New York: Dover.

Kunz, K., Reiter, J., Götzelmann, A. & Stamm, M. (1993). *Macromolecules*, **26**, 4316–4323.

Lee, E. M. & Milnes, J. S. (1995). *J. Appl. Cryst.* **28**, 518–526.

Lekner, J. (1987). *Theory of Reflection*. Dordrecht: Nijhoff.

Lekner, J. (1991). *Physica (Utrecht)*, B**173**, 99–111.

Li, Z. X., Lu, J. R., Styrkas, D. A., Thomas, R. K., Rennie, A. R. & Penfold, J. (1993). *Mol. Phys.* **80**, 925–939.

Lu, J. R., Hromadova, M., Simister, E. A., Thomas, R. K. & Penfold, J. (1994). *J. Phys. Chem.* **98**, 11519–11526.

Lu, J. R., Hromadova, M. & Thomas, R. K. (1993). *Langmuir*, **9**, 2417–2425.

Lu, J. R., Lee, E. M., Thomas, R. K., Penfold, J. & Flitsch, S. (1993). *Langmuir*, **9**, 1352–1360.

Lu. J. R., Li, Z. X., Smallwood, J. A., Thomas, R. K. & Penfold, J. (1995). *J. Phys. Chem.* **99**, 8233–8243.

Lu, J. R., Li, Z. X., Su, T. J., Thomas, R. K. & Penfold, J. (1993). *Langmuir*, **9**, 2408–2416.

Lu, J. R., Li, Z. X., Thomas, R. K., Staples, E. J., Thompson, L., Tucker, I. & Penfold, J. (1994). *J. Phys. Chem.* **98**, 6559–6567.

Lu, J. R., Li, Z. X., Thomas, R. K., Staples, E. J., Tucker, I. & Penfold, J. (1993). *J. Phys. Chem.* **97**, 8012–8020.

Lu, J. R., Simister, E. A., Lee, E. M., Thomas, R. K., Rennie, A. R. & Penfold, J. (1992). *Langmuir*, **8**, 1837–1844.

Lu, J. R., Simister, E. A., Thomas, R. K. & Penfold, J. (1993*a*). *J. Phys. Chem.* **97**, 6024–6033.

Lu, J. R., Simister, E. A., Thomas, R. K. & Penfold, J. (1993*b*). *J. Phys. Chem.* **97**, 13907–13913.

Lu, J. R. & Thomas, R. K. (1995). *Nucl. Instrum.* A**354**, 149–163.

McDermott, D. C., McCarney, J., Thomas, R. K. & Rennie, A. R. (1994). *J. Colloid Interface Sci.* **304**, 304–310.

Nevot, L. & Croce, P. (1980). *Rev. Phys. Appl.* **15**, 761–779.
Parratt, L. G. (1954). *Phys. Rev.* **95**, 359–369.
Pedersen, J. S. (1992). *J. Appl. Cryst.* **25**, 129–145.
Pedersen, J. S. & Hamley, I. W. (1994*a*). *J. Appl. Cryst.* **27**, 36–49.
Pedersen, J. S. & Hamley, I. W. (1994*b*). *Physica (Utrecht)*, B**198**, 16–23.
Penfold, J. & Thomas, R. K. (1990). *J. Phys. Condens. Matter*, **2**, 1369–1412.
Penfold, J., Webster, J. R. P., Bucknall, D. G. & Sivia, D. S. (1994) *Colloid Surf.* **86**, 165–169.
Pershan, P. S. (1989). *J. Phys. (Paris) Colloq.* C-**7**, 1–20.
Pershan, P. S. (1994*a*). *J. Phys. Condens. Matter*, **23**A, A37–A50.
Pershan, P. S. (1994*b*). *Phys. Rev. E*, **50**, 2369–2372.
Reynolds, G. O., DeVelis, J. B., Parrent, G. B. & Thompson, B. J. (1989). *Tutorials in Fourier Optics*. Washington: International Society for Optical Engineering.
Russell, T. P. (1990). *Mater. Sci. Rep.* **5**, 171–271.
Sanyal, M. K., Sinha, S. K., Gibaud, A., Huang, K. C., Carvalho, B. L., Rafailovich, M., Sokolov, J., Zhao, X. & Zhao, W. (1993). *Europhys. Lett.* **21**, 691–696.
Schlossman, M. L. & Pershan, P. S. (1992). In *Light Scattering by Liquid Surfaces and Complementary Techniques*, edited by D. Langevin. New York: Dekker.
Schlossman, M. L., Schwartz, D. K., Kawamoto, E. H., Kellogg, G. J., Pershan, P. S., Kim, M. W. & Chung, T. C. (1991). *J. Phys. Chem.* **95**, 6628–6632.
Schwartz, D. K., Schlossman, M. L., Kawamoto, E. H., Kellogg, G. J., Pershan, P. S. & Ocko, B. M. (1990). *Phys. Rev. A*, **41**, 5687–5690.
Sears, V. F. (1989). *Neutron Optics*. Oxford University Press.
Simister, E. A., Lee, E. M., Thomas, R. K. & Penfold, J. (1992*a*). *Macromol. Rep.* A**29**, 155–162.
Simister, E. A., Lee, E. M., Thomas, R. K. & Penfold, J. (1992*b*). *J. Phys. Chem.* **96**, 1373–1382.
Singh, N., Tirrell, M. & Bates, F. S. (1993). *J. Appl. Cryst.* **26**, 650–659.
Sinha, S. K., Sirota, E. B., Garoff, S. & Stanley, H. B. (1988). *Phys. Rev. B*, **38**, 2297–2308.
Sivia, D. S., Hamilton, W. A. & Smith, G. S. (1991). *Physica (Utrecht)*, B**173**, 121–138.
Styrkas, D. A. (1994). DPhil thesis, University of Oxford, England.
Styrkas, D. A., Thomas, R. K., Adib, Z. A., Davis, F., Hodge, P. & Liu, X. H. (1994). *Macromolecules*, **27**, 5504–5510.
Thomas, R. K. (1995). In *Scattering Methods in Polymer Science*, edited by R. W. Richards. London: Ellis Horwood.
Vaknin, D., Als-Nielsen, J., Peipenstock, M. & Losche, M. (1991). *Biophys. J.* **60**, 1545–1550.
Zhou, X. L. & Chen, S. H. (1993). *Phys. Rev. E*, **47**, 3174–3190.
Zhou, X. L. & Chen, S. H. (1995). *Phys. Rep.* **257**, 226–348.
Zhou, X. L., Chen, S. H. & Felcher, G. P. (1992). *Phys. Rev. E*, **46**, 1839–1843.
Zhou, X. L., Lee, L. T., Chen, S. H. & Strey, R. (1992). *Phys. Rev. A*, **46**, 6479–6489.